

A NEW APPROACH TO 3-DIMENSIONAL OPTIMIZATION OF ULTIMATE  
PIT GEOMETRY FOR OPEN PIT MINES WITH VARIABLE OVERALL SLOPE  
ANGLES

A THESIS SUBMITTED TO  
THE GRADUATE SCHOOL OF NATURAL AND APPLIED SCIENCES  
OF  
MIDDLE EAST TECHNICAL UNIVERSITY

BY

FİRDEVS KÜBRA ALTUNTOV

IN PARTIAL FULFILLMENT OF THE REQUIREMENTS  
FOR  
THE DEGREE OF MASTER OF SCIENCE  
IN  
MINING ENGINEERING

SEPTEMBER 2019



Approval of the thesis:

**A NEW APPROACH TO 3-DIMENSIONAL OPTIMIZATION OF  
ULTIMATE PIT GEOMETRY FOR OPEN PIT MINES WITH VARIABLE  
OVERALL SLOPE ANGLES**

submitted by **FİRDEVS KÜBRA ALTUNTOV** in partial fulfillment of the requirements for the degree of **Master of Science in Mining Engineering Department, Middle East Technical University** by,

Prof. Dr. Halil Kalıpçılar  
Dean, Graduate School of **Natural and Applied Sciences**

\_\_\_\_\_

Prof. Dr. Celal Karpuz  
Head of Department, **Mining Engineering**

\_\_\_\_\_

Assist. Prof. Dr. Mustafa Erkayaoğlu  
Supervisor, **Mining Engineering, METU**

\_\_\_\_\_

**Examining Committee Members:**

Prof. Dr. Celal Karpuz  
Mining Engineering, METU

\_\_\_\_\_

Assist. Prof. Dr. Mustafa Erkayaoğlu  
Mining Engineering, METU

\_\_\_\_\_

Assoc. Prof. Dr. İ. Ferid Öge  
Mining Engineering, MSKU

\_\_\_\_\_

Date: 02.09.2019

**I hereby declare that all information in this document has been obtained and presented in accordance with academic rules and ethical conduct. I also declare that, as required by these rules and conduct, I have fully cited and referenced all material and results that are not original to this work.**

Name, Surname: Firdevs Kübra Altuntov

Signature:

## **ABSTRACT**

### **A NEW APPROACH TO 3-DIMENSIONAL OPTIMIZATION OF ULTIMATE PIT GEOMETRY FOR OPEN PIT MINES WITH VARIABLE OVERALL SLOPE ANGLES**

Altuntov, Firdevs Kübra  
Master of Science, Mining Engineering  
Supervisor: Assist. Prof. Dr. Mustafa Erkayaoğlu

September 2019, 105 pages

The mining activities have high economic risks and the determination of the optimum ultimate pit limit of an ore body greatly affects the economic feasibility of an open pit mine. Due to necessity of determining optimum pit limit, many researchers proposed different algorithms and heuristic methods which maximize economic value of a mine while satisfying operational constraints and extraction sequence constraints. In most of the proposed methods, overall slope angle variation in the pit is constant. However, in real situations, overall slope angle varies in different parts of the mine due to geotechnical reasons. Since overall slope angle is an important constraint in open pit optimization and it is a significant factor in terms of slope stability, overall slope angle variation should be taken into consideration in optimization algorithms. In previous studies, methods that include overall slope angle variation were generally formed according to precedence relationships among blocks, but these methods also have problems in creating variable overall slope angles. To overcome this problem, in this study, it is aimed to apply a new approach which includes overall slope angle variation in optimization of ultimate pit limits. For this purpose, mixed integer programming and cubic spline interpolation were utilized, and the application was performed by

coding in Python Programming Language. The proposed method was verified by applying it to the four case studies.

Keywords: Optimum Ultimate Pit Limit, Open Pit Mining, Overall Slope Angle, Spline Interpolation

## ÖZ

### DEĞİŞKEN GENEL ŞEV AÇILI AÇIK OCAKLAR İÇİN 3 BOYUTLU NİHAİ OCAK GEOMETRİSİNİN OPTİMİZASYONU İÇİN YENİ BİR YÖNTEM

Altuntov, Firdevs Kübra  
Yüksek Lisans, Maden Mühendisliği  
Tez Danışmanı: Dr. Öğr. Üyesi Mustafa Erkayaoğlu

Eylül 2019, 105 sayfa

Madencilik yüksek ekonomik risk taşıyan bir sektördür ve cevher yataklarının en uygun nihai ocak sınırlarının belirlenmesi, açık ocak madenlerinin fizibilitesini önemli derecede etkiler. En uygun nihai ocak sınırın belirlenmesinin gerekliliğinden dolayı, birçok araştırmacı operasyonel ve cevher bloklarını çıkarma sırası gibi kısıtlamaları ihlal etmeden ekonomik değeri maksimum seviyeye çıkaran farklı algoritmaları ve sezgisel yöntemleri ileri sürmüşlerdir. Öne sürülen yöntemlerin çoğunda, açık ocaktaki genel şev açısı değişimi sabittir; ama gerçek durumlarda maden ocağının farklı bölümlerinde şev açısı jeoteknik nedenlerden dolayı değişkendir. Genel şev açısı optimizasyonda önemli bir kısıtlama olduğundan ve şev duraylılığı için önemli olduğundan, genel şev açısı değişimi optimizasyon algoritmalarında dikkate alınmalıdır. Önceki araştırmalarda, genel şev açısı değişimini içeren yöntemler genellikle blokların çıkarılma önceliği dikkate alınarak oluşturulmuştur; ama bu yöntemler de değişken genel şev açılarını dahil etme bakımından yetersizdir. Bu probleme bir çözüm olarak, bu çalışmada genel şev açısı değişimini içeren yeni bir yöntemin uygulanması amaçlanmıştır. Bu tekniği uygulamak için, karma tamsayılı programlama ve kübik spline interpolasyonu kullanılmıştır. Bu teknik için Python

programlama dili kullanılarak kod yazılmıştır. Önerilen yöntem dört açık ocak üzerinde uygulanarak doğrulanmıştır.

Anahtar Kelimeler: Optimum Nihai Ocak Sınırı, Açık Ocak Madenciliği, Genel Ocak Eğim Açısı, Spline İnterpolasyonu

To My Family

## **ACKNOWLEDGEMENTS**

I would like to express my appreciation and gratitude to Assist. Prof. Dr. Mustafa Erkayaođlu and Prof. Dr. Celal Karpuz for their guidance and encouragement. The completion of this thesis could not have been possible without their expertise and support.

I would like to thank the examining committee member Assoc. Prof. Dr. İ. Ferid Öge for his valuable contributions.

## TABLE OF CONTENTS

ABSTRACT .....	v
ÖZ .....	vii
ACKNOWLEDGEMENTS .....	x
TABLE OF CONTENTS .....	xi
LIST OF TABLES .....	xiv
LIST OF FIGURES .....	xvi
CHAPTERS	
1. INTRODUCTION .....	1
1.1. Problem Statement .....	1
1.2. Aim and Scope of the Study .....	1
1.3. Thesis Outline.....	2
2. LITERATURE REVIEW .....	3
2.1. Ultimate Pit Limit.....	3
2.2. Long-term Production Planning .....	9
3. METHODOLOGY .....	17
3.1. Basic Terminology for Surface Mining.....	17
3.2. Block Modeling and Economic Block Value .....	18
3.2.1. Grade Assignment to Blocks .....	18
3.2.2. Economic Block Value .....	21
3.3. Geotechnical Slope Design.....	22

3.3.1. Limit Equilibrium Method .....	22
3.3.2. Numerical Analysis .....	23
3.3.3. Probabilistic Approach .....	23
3.4. Incorporation of Slope Design in Open Pit Optimization.....	23
3.4.1. Spline Interpolation .....	25
4. ALGORITHM DEVELOPMENT .....	33
4.1. Incorporation of Overall Slope Angles in the Model.....	35
4.2. Mixed Integer Programming .....	40
4.3. Verification of the Algorithm .....	43
5. THE GRAPHICAL USER INTERFACE .....	57
5.1. GUI for Input Data.....	57
5.2. GUI for Output Data .....	63
6. CASE STUDY .....	69
6.1. Magnetite Orebody .....	69
6.1.1. Block Model .....	69
6.1.2. Economic Block Value and Input Data .....	70
6.1.3. Results .....	71
6.2. Magnetite-hematite Orebody .....	73
6.2.1. Block Model .....	73
6.2.2. Economic Block Values and Input Data .....	74
6.2.3. Results .....	75
6.3. Lignite Orebody 1 .....	77
6.3.1. Block Model .....	77
6.3.2. Economic Block Values and Input Data .....	78

6.3.3. Results.....	79
6.4. Lignite Orebody 2 .....	81
6.4.1. Economic Block Values and Input Data.....	81
6.4.2. Results.....	82
7. CONCLUSION AND RECOMMENDATIONS .....	85
REFERENCES.....	89
APPENDICES	
A. PSEUDOCODE FOR SPLINE INTERPOLATION.....	97
B. RESULTS OF THE ITERATIONS FOR THE CASE STUDIES .....	99
C. OVERALL SLOPE ANGLES AND CROSS SECTIONS .....	101

## LIST OF TABLES

### TABLES

Table 3.1. Different overall slope angles for different azimuths.....	29
Table 3.2. Corresponding x and y coordinates of the points given in the Table 3.1 .	29
Table 4.1. Input values.....	46
Table 4.2. Block dimensions .....	46
Table 4.3. Number of blocks .....	46
Table 4.4. Comparison of overall slope angles for the first example .....	48
Table 4.5. Overall slope angle inputs for the second example .....	49
Table 4.6. Comparison of overall slope angles for the second example .....	50
Table 4.7. Input values for the third example.....	51
Table 4.8. Comparison of overall slope angles for the third example.....	51
Table 4.9. Overall slope angles for the fourth example.....	52
Table 4.10. Comparison of overall slope angles for the fourth example.....	54
Table 6.1. Number of blocks .....	69
Table 6.2. Output data .....	72
Table 6.3. Number of blocks .....	73
Table 6.4. Overall slope angles.....	75
Table 6.5. Output data .....	77
Table 6.6. Number of blocks .....	77
Table 6.7. Input data for depth ranges .....	79
Table 6.8. Output data .....	80
Table 6.9. Input data for depth range, overall slope angle, and azimuth.....	81
Table 6.10. Output data .....	83
Table B.1. Case study 1 .....	99
Table B.2. Case study 2 .....	99
Table B.3. Case study 3 .....	100

Table B.4. Case study 4.....	100
Table C.1. Overall slope angles for smaller block model (number of blocks =81,600) .....	101
Table C.2. Overall slope angles for larger block model (number of blocks=494,900) .....	102
Table C.3. Comparison of overall slope angles for magnetite orebody.....	103
Table C.4. Comparison of overall slope angles for magnetite-hematite orebody....	104
Table C.5. Comparison of overall slope angles for lignite orebody (lignite 1) .....	105
Table C.6. Comparison of overall slope angles for lignite orebody (lignite 2) .....	105

## LIST OF FIGURES

### FIGURES

Figure 3.1. Bench geometry.....	17
Figure 3.2. A spherical model of semi-variogram (Hustrulid et al., 2013) .....	21
Figure 3.3. Precedence in extraction of blocks a) 1-5 Pattern b) 1-9 Pattern .....	24
Figure 3.4. Shapes of cones formed by (a) linear and (b) spline interpolation (Sattarvand & Shisvan, 2012).....	25
Figure 3.5. Shapes constructed with a) quadratic spline b) cardinal spline c) cubic spline (Sattarvand & Shisvan, 2012) .....	26
Figure 3.6. A segment of curve from point $P_k$ to $P_{k+1}$ .....	27
Figure 3.7. Cone template's a) isometric, b) top, and c) side view .....	28
Figure 3.8. Points created by spline interpolation in plan view.....	30
Figure 3.9. Five levels of points created by spline interpolation in plan view .....	31
Figure 4.1. Pseudo-code for the main steps of the algorithm .....	35
Figure 4.2. Radius of a block and other parameters in cross-sectional view.....	37
Figure 4.3. Radius of a block in plan view .....	37
Figure 4.4. Different overall slope angles in different azimuth directions .....	38
Figure 4.5. Plan view of the pit shape in Figure 4.4 .....	38
Figure 4.6. Different overall slope angles in different depth ranges .....	39
Figure 4.7. Plan view of the pit shape given in Figure 4.6 .....	39
Figure 4.8. A section of a pit .....	42
Figure 4.9. A section of a pit with different slope angle .....	43
Figure 4.10. Extracted blocks with $45^\circ$ overall slope .....	44
Figure 4.11. Section view of the block model .....	44
Figure 4.12. Cross-section “A-A” .....	45
Figure 4.13. Selected blocks .....	45
Figure 4.14. Constant overall slope angle .....	47

Figure 4.15. W-E section of the extracted blocks for the first example.....	47
Figure 4.16. N 10 E section of the extracted blocks for the first example.....	47
Figure 4.17. Extracted blocks of the second example.....	48
Figure 4.18. Curve created by using spline interpolation for the second example ....	49
Figure 4.19. N 40 E section of the extracted blocks for the second example .....	50
Figure 4.20. S 30 W section of the extracted blocks for the second example .....	50
Figure 4.21. Extracted blocks of the third example .....	51
Figure 4.22. W-E section of the extracted blocks for the third example .....	52
Figure 4.23. N 40 E section of the extracted blocks for the third example.....	52
Figure 4.24. Curve created by using spline interpolation for the fourth example ....	53
Figure 4.25. Extracted blocks of the fourth example (lignite deposit).....	53
Figure 4.26. N 45 E section of the extracted blocks for the fourth example .....	54
Figure 4.27. S 45 E section of the extracted blocks for the fourth example .....	54
Figure 4.28. Comparison between input and output values of overall slope angles of the block models with large and small number of blocks.....	55
Figure 5.1. Entry window for data input.....	58
Figure 5.2. Case 1: Entry window for overall slope angle.....	59
Figure 5.3. Case 2: Entry window for number of zones .....	59
Figure 5.4. Case 2: Entry window for overall slope angles in different azimuth ranges .....	60
Figure 5.5. Case 3: Entry window for number of zones .....	60
Figure 5.6. Case 3: Entry window for overall slope angles in different ranges of depth .....	61
Figure 5.7. Case 4: Entry window for number of zones for azimuth and depth .....	61
Figure 5.8. Case 4: Entry window for overall slope angles in different azimuth ranges .....	62
Figure 5.9. Case 4: Entry window for ranges of depth .....	63
Figure 5.10. Ultimate pit limit of a block model consisting of 125,000 blocks .....	65
Figure 5.11. Extracted blocks of a block model consisting of 125,000 blocks .....	66

Figure 5.12. The points created by cubic spline interpolation for various overall slope angles .....	67
Figure 5.13. Information window for total economic block value and stripping ratio .....	68
Figure 6.1. Block model of the magnetite orebody .....	70
Figure 6.2. Economic block value parameters for case 1 .....	71
Figure 6.3. Extracted blocks .....	72
Figure 6.4. N-S section of the extracted blocks .....	72
Figure 6.5. Block model of the magnetite-hematite orebody .....	73
Figure 6.6. Economic block value and bench parameters for case 2.....	74
Figure 6.7. The curve formed by spline interpolation for case 2.....	75
Figure 6.8. Extracted blocks .....	76
Figure 6.9. N 45 E section of the extracted blocks .....	76
Figure 6.10. Block model of the lignite orebody.....	78
Figure 6.11. Economic block value and bench parameters for case 3.....	79
Figure 6.12. Extracted blocks .....	80
Figure 6.13. N-S section of the extracted blocks .....	80
Figure 6.14. The curve formed by spline interpolation for case 4.....	82
Figure 6.15. Extracted blocks .....	83
Figure 6.16. N 45 E section of the extracted blocks .....	83
Figure C.1. N 45 E section of the extracted blocks of the magnetite orebody .....	103
Figure C.2. W E section of the extracted blocks of the magnetite orebody .....	103
Figure C.3. S 45 E section of the extracted blocks of magnetite-hematite orebody	104
Figure C.4. N 45 E section of the extracted blocks of lignite orebody (lignite 1)...	104
Figure C.5. W E section of the extracted blocks of lignite orebody (lignite 1).....	104
Figure C.6. S 45 E section of the extracted blocks for lignite orebody (lignite 2) ..	105

# CHAPTER 1

## INTRODUCTION

### 1.1. Problem Statement

It becomes crucial to find the optimum pit limits that will provide the most profitable outcome as the deposits are becoming rare. The selection of the method that will be used for the optimization is important to obtain maximum economic value. However, importance must be also given to geotechnical aspects to ensure that safety requirements are met. Thus, overall slope angles must be incorporated in the optimization process. In this study, previous studies are examined to see how overall slope angles are included in the design. In the conventional methods, there are problems in acquiring different overall slope angles. In addition, overall slope angles are included in the design after the completion of optimization procedure. It is better to incorporate the slope angles in the optimization process for optimum results. Thus, a new approach must be proposed to include geotechnical constraints in the optimization.

### 1.2. Aim and Scope of the Study

The aim of this thesis is to apply a new technique in which optimum ultimate pit limit is determined by ensuring preset overall slope angles are obtained. To achieve this objective, the mathematical model is formed, and the model is coded in the Python Programming Language. In addition, graphical user interface is coded so that economic block value parameters, bench slope angle, bench height, overall slope angles can be entered. The optimization method that is utilized is mixed integer programming and the technique that is used for generating various overall slope angles is cubic spline interpolation. The result generated by the code gives total economic block value, depth of the pit, maximum radius of the pit and the stripping ratio.

In this study, undiscounted value of money is used in the calculation of economic block value. It would be more realistic if time value of money was considered. However, to apply a new approach for various overall slope angles, first step of open pit optimization that is determining ultimate pit limit is chosen to be studied because of its simplicity compared to other stages such as push back design and production planning.

### **1.3. Thesis Outline**

In Chapter 1, purpose and scope of the thesis are explained. In Chapter 2, literature review on ultimate pit limit and long-term production planning is provided. In Chapter 3, basic terms used in surface mining are defined. In addition, block modeling, economic block value calculation, and geotechnical design are briefly explained. Detailed explanation about spline interpolation are provided to explain how open pit shape is created with given overall slope angles. In Chapter 4, the proposed algorithm is explained. Main steps of the algorithm are given as a pseudo-code. Objective function of mixed integer programming, incorporation of slope angles in the objective function, and validation of the algorithm are presented. Chapter 5, the graphical user interface that is created are demonstrated and how to use the interface is explained. In Chapter 6, 4 case studies are presented. In Chapter 7, conclusions and recommendations are provided.

## CHAPTER 2

### LITERATURE REVIEW

In open pit mining, optimization for production planning consist of mainly three stages which are determining ultimate pit limit, generating nested pits and pushbacks, and block sequencing. Production planning can be considered in three stages if the time span is considered. For long-term planning, the extraction sequence is mostly determined in years. For the medium-term planning, the time span is one year, and the sequences are grouped in monthly or quarterly periods. The short-term planning has a monthly time span and the sequence of operations for each week, day or shift is determined (Auger, 2000). In this chapter, researches on optimization techniques for final pit limit and long-term production planning are presented.

#### 2.1. Ultimate Pit Limit

Ultimate pit limit represents the geometrical outline of the mine at the end of its economic life. Generally, optimum ultimate pit limit is found without considering time value of money, but in some techniques, ultimate pit limit and long-term production plan are simultaneously determined considering time value of money. If optimum ultimate pit limit is found before long-term production is planned, determining final pit outline makes it easier to organize short, medium, and long-term exploitation sequences by decreasing the complexity of the problem (Noghli, 2015). Several researchers attempted to develop algorithms or heuristics methods to solve ultimate pit limit problem. Some of the proposed methods are dynamic programming, methods in graph theory, moving cone method, genetic algorithm, and stochastic approaches.

Dynamic programming is an approach of solving complex problems by turning the problem into assembly of simpler problems. In 1965, the dynamic programming to solve final pit limit problem was firstly presented by Lerchs and Grossmann (Noghli,

2015). Although the algorithm guarantees an optimal solution, this algorithm was developed for two dimensional problems. Johnson and Sharp (1971) improved this method so that the algorithm can be applied to 3D open pit geometry. However, these developed algorithms could not prevent suboptimum results (Erarslan, 1996). In 1982, Koenigsberg adapted the 2D algorithm to 3D open pits. The major drawback of the algorithm was stated to be the possibility of creating inconsistency between blocks. Thus, slope requirement may not be achieved (Asa, 2002). In addition, according to Shenggui and Starfield (1985), degeneration can happen in the Koenigsberg algorithm, which may lead to not achieving optimal result because it is over-constrained. Furthermore, the model developed by Koenigsberg (1982) is not suitable for large-sized block models (Noghli, 2015).

In order to further improve dynamic programming, Wilke and Wright (1984) introduced a new procedure combining dynamic programming and minimum removal of cones. It was a successful application, but it presents a trade-off situation such that if 2D dynamic programming with cones is used, the algorithm becomes over-constrained; if 2D dynamic programming without cones is used, smoothing is required (Milani, 2016). To sort out smoothing problem, a method was presented by Z. Shenggui, and A.M. Starfield (1985). However, it is a heuristic method, i.e. it does not guarantee optimal solution (Milani, 2016). In 1987, Koenigsberg made changes in the algorithm to reduce time of solution, but these modifications do not render the solution optimal (Auger,2000).

The first algorithm in 3D for ultimate pit limit problem was developed by Lerchs and Grossmann in 1965. Lerchs and Grossmann's algorithm yields an optimum solution. However, the algorithm required an unpractical solution time and computer memory in the past. Thus, previous researches mainly focused on reducing solution time by limiting number of blocks included in the computation. Rychkun and Chen (1979), Barnes and Johnson (1982) proposed bounding methods to decrease number of blocks to increase solution speed (Huttagosol, 1988). In 1988, Huttagosol modified Lerchs and Grossmann algorithm by changing tree configuration so that requirement for

computer memory and solution time can be reduced. Lipkewich and Borgman (1969), Chen (1977), Stuart (1992), Zhao and Kim (1992) attempted to overcome certain limitations, such as incorporating slope angle and haulage roads, and reducing time of solution.

Dowd and Onur (1993), Zhao and Kim (1992) deployed cone templates for variable slope angles where only a single slope angle was defined (Khalokakaie, 1999).

Lipkewich and Borgman (1969) used knight move pattern. In 1999, Khalokakaie published a study in which variable slopes were incorporated in the algorithm of Lerchs and Grossmann. To develop a technique for variable overall slope angles, the method proposed by Dowd and Onur (1993) was adapted to the method introduced by Khalokakaie. In this research, the orebody is divided into four principle directions in which different slope angle requirements are present and changes in overall slope angle with respect to depth is taken into account by using equation of an ellipse geometry.

Floating cone method is a heuristic method that is easy to apply and requires low amount of computing time compared to other methods. Despite of its advantages, this technique does not necessarily produce optimum results. Thus, various researchers introduced variations of this method to tackle with suboptimal results. The first floating cone method was proposed by Pana et al (1965). In this floating cone technique, procedure starts from the first level. Positive blocks are searched on every level. If there is a positive block on a level, a cone is formed. If the value of that cone is positive, then the cone is extracted. To improve this technique, in 1999, Wright modified this method and proposed a method called floating cone 2. In this technique, cone values of positive blocks are found and cone values are cumulatively added to the value of the cone with maximum value. The cone with the highest cumulative value is extracted. The procedure is repeated on each level.

Elahizeyni et al. (2011) introduced floating cone 3 method and claimed that their proposed method gives better results compared to other floating cone methods and the result obtained from Lerch and Grossmann algorithm is similar to the result obtained from floating cone 3 method.

In 1968, Johnson demonstrated the relationship between ultimate pit limit problem and the maximum flow. In this study, outlines created by Lerchs and Grossmann are used on a bipartite graph. The bipartite graph is formed in a such a way that an arc is created if there is a direct path between a positive and negative weighted node. According to Hochbaum and Chen (2000), Johnson (1968) depicted the problem of ultimate contours as a transport problem and he stated that this problem could be solved as a maximum flow problem. In 1976, Picard mathematically demonstrated that the method presented by Lerchs and Grossmann was equivalent to finding a maximum flow on a graph adapted to the problem of ultimate limit. The network constructed by Picard is adapted from Lerchs and Grossmann's graph and is obtained by adding a source and sink node. Tachefine et al. (1993), and Hochbaum and Chen (2000) conducted efficiency tests to determine whether the maximum flow algorithm is the most effective way for resolving this type of problem. According to the results provided by Hochbaum and Chen, push-relabel algorithm was the most promising algorithm. Tachefine claimed that Highest Label Preflow Algorithm is the most efficient algorithm for solving the maximum flow problem on the graphs representing mineral deposits. Giannini (1990) demonstrated that Lerchs and Grossmann's algorithm is equivalent to Dual Simplex Linear Programming and stated that using network flow method is more practical than using these algorithms. Underwood and Tolwinski (1998) employed mathematical programming and graph theory together applying dual simplex method. Hochbaum and Chen (2000) proposed maximum flow push-relabel algorithm. In 2010, Hochbaum proposed a method called pseudoflow algorithm in order to solve maximum flow problem. Abbaspour (2011) claimed that Lerchs and Grossmann's algorithm is equivalent to pseudoflow algorithm proposed by Hochbaum, and found that it is faster than Lerchs and Grossmann's algorithm.

Some heuristic methods were introduced by many researchers to deal with the drawbacks of conventional methods to determine ultimate pit limit. Some of these methods are genetic algorithm and artificial neural network.

Genetic algorithm is an optimization technique inspired by genetics and natural selection. In genetic algorithm, individuals of a population evolve to a state in which the fitness of the individuals are maximum (Haupt & Haupt, 2004). Concepts of crossover of genes, mutation, and survival of the fittest are implemented in this algorithm. Basically, in genetic algorithm, random solutions (individuals) are generated in order to maximize the objective function (fitness of the individual), and among these solutions, a pair of solution is selected based on their fitness value. Then, chromosomes of the selected pair are combined by crossover. In addition, offspring of the pair is mutated depending on the predetermined probability. This process is repeated until the preset number of generations is reached. According to Haupt and Haupt (2004), some of the advantages of genetic algorithm are that:

- it can handle large number of variables.
- it can generate a list of feasible solutions, not just one solution
- it can provide solution of complex surfaces because it can jump out of local minimum or maximum.
- parallel computing can be performed.

To determine optimum pit limit and to cope with drawbacks of other open pit optimization techniques, in 2016, Milani proposed a non-standard genetic algorithm with zooming strategy for 2D and 3D pit layouts. Zooming is forming elite group of individuals which have high fitness in a population. According Milani (2016), the proposed genetic algorithm requires less computational effort compared with other conventional methods of open pit optimization and reruns should be performed in order to prevent suboptimal solutions. Although this genetic algorithm provides many advantages, desired overall slope angle may not be acquired but various slope angles can be formed only between the blocks.

Not including stochastic properties of ore grade and commodity prices in pit limit optimization can also lead to a suboptimal result. To handle this problem, Achireko (1998) proposed an algorithm in which artificial neural network is used. In the proposed algorithm, to model ore grade and reserve, modified conditional simulation is used and multilayer feedforward neural networks are used to classify blocks according to conditioned values. In addition, to model commodity prices, multiple regression model and multilayer feedforward neural network are used. In the algorithm, variable slope angles are incorporated. To verify their algorithm, they compared their algorithm with the results of Lerchs-Grossman's algorithm and the results are similar if there are no blocks having zero value. They claim that their algorithm generates results faster than Lerchs-Grossman's algorithm. However, according to Sayadi et al. (2011), the algorithm requires modifications because of mainly 3 reasons. Firstly, smoothing is required. To deal with smoothing problem, the algorithm needs to be modified to obtain 3D pit layouts. Secondly, in large scale orebodies, the neural network error can have considerable effect on results. Finally, slope constraints in the algorithm can cause undesired block selections. To sort out these problems, Sayadi et al. (2011) proposed a new 3D pit optimization algorithm in which artificial neural network is used to find the ultimate pit limit. The algorithm consists of 3 stages. In the first stage, economic block model is created. In the second stage, artificial neural network is used to classify blocks into positive and negative regions. Neural network input is x, y, z coordinates of blocks and economic block values. The neural network output is block value. Block value is assigned as 1 if economic value is higher than 0; otherwise it is assigned as -1. In the third stage, the blocks in the positive region are checked, and slope constraint and grade constraint are taken into account. The results obtained from the algorithm is compared with that from the modified Lerchs-Grossman's algorithm. The results are similar to each other, but the algorithm produces higher profit if ore impurity constraint is included in the algorithm.

## **2.2. Long-term Production Planning**

Production planning for operations in an open pit mine is defined as planning the sequence of exploitation from the initial state of the deposit to its final state or the final contours of the pit. Many researchers proposed algorithms or heuristics method for long-term production planning. Some of the developed techniques are linear programming, mixed integer programming, integer programming, dynamic programming, parameterization, positional weight technique, aggregation, genetic algorithm, and simulated annealing.

In 1969, linear programming was firstly used by Johnson for production planning. The proposed mathematical model includes time value of money, processing constraints, dynamic cutoff grade. This mathematical model represents a large multi-period problem. In this model, the main problem is turned into smaller problems. Every subproblem is solved as a single period problem and optimum limits are found. To find the ultimate pit limit, maximum network flow can be used. After solving all the subproblems, solving the main problem becomes relatively easy (Özkan, 2015). This method can give solutions for each subproblem, but it has drawbacks in solving long-term production planning problem. It produces fractional solutions between 0 and 1. In addition, it creates solutions in which underlying blocks are extracted before overlying blocks are extracted. This leads to some parts of a block appear as an air block (Osanloo et al., 2008).

To overcome the disadvantages in modeling the problem by using linear programming, Gershon (1983) proposed a mixed integer programming. By this using method, the problem that underlying blocks are extracted before overlying block is sorted out. However, problem size of mixed integer programming is too large to be solved by commercial software programs (Özkan, 2015). To solve this kind of problems, the problem is converted into subproblems. For example, finding ultimate pit limit before designing production sequence decreases number of blocks that are dealt with. This consequently decreases time of computation (Caccetta and Hill,

2003). This approach has two advantages compared to linear programming. Firstly, it provides more applicable extraction sequence. Second advantage is that before extracting one underlying block, overlying blocks must be removed. Disadvantage of this method is that commercial software programs cannot be used for large-sized problems because the model has a lot of binary variables (Özkan, 2015). In addition, dynamic cutoff grade is not included in the calculation due to large model size (Osanloo et al., 2008). Integer programming is also used for production planning, but large model size creates problem in finding a solution (Khan and Niemann-Delius, 2014).

Liu & Kozan (2016) stated that exact mixed integer programming optimizers and relaxation methods of mixed integer programming presents difficulties when it comes to solving large scale problems. In metaheuristics, unexpected randomness which is the characteristic attribute of metaheuristics and not using important features associated with production scheduling may also create problems. Because of these reasons, Liu & Kozan (2016) introduced two new graph-based algorithms. These algorithms consist of network flow graph and scheduling theory. One of the algorithms produces more optimal solution but it requires higher computation time. According to Liu & Kozan (2016), the proposed algorithms are better at performance compared to other methods of production scheduling because mixed integer programming optimizer and random neighborhood search is not required in the algorithm.

Since long-term planning can be divided into smaller problems, dynamic programming can be used. Thus, many researches proposed dynamic programming for production planning. In production planning, dynamic programming was firstly used by Roman (1974). Finding ultimate pit limit and extraction sequence are simultaneously determined in this method. In this algorithm, the last block extracted must be determined at the beginning of the calculation. The overlying blocks above the chosen blocks are checked considering slope angles. Optimum extraction sequence is determined based on net present value. The sequence which gives the maximum net present value is selected and it is combined with the pit shape formed at the beginning.

Blocks contributing negative net present value are excluded from the ultimate limit and they are not included in the production planning. In this procedure, every block is checked. Advantage of this method is that ultimate pit limit is found by including time value of money and block extraction sequence. Disadvantage of this method is that it is hard to apply the method to large scale models due to complexity of the method. In addition, constraints for excavation capacity and processing are not guaranteed to be satisfied (Özkan, 2015).

Dowd and Onur (1992), Dowd and Onur (1993) also proposed a dynamic programming method and they stated that computer capacities are insufficient in solving large-sized problems since this method produces many alternatives. However, they stated that due to different constraints in production planning, extremely high number of alternatives decreases. In the beginning of the algorithm, stages are formed by dividing the production operations into periods. In this algorithm, sequences in the given stages are found.

Erarslan and Celebi (2001) developed a simulation and optimization model which determines ultimate pit limit as a function of production planning. In this method, economic value of the blocks is calculated based on the size of the pit. Variables such as excavator movements, slope stability, processing capacity and time value of money are included in the method. In this technique, optimum pit limit is the pit shape which gives the maximum net present value. The algorithm firstly determines the ultimate pit limit. This limit is accepted as the largest limit possible. After that, unit cost is calculated. After the starting point of the excavation is determined, block extraction sequence is simulated in the 3D coordinate system. Operational constraints such as excavation activities, blending, stocking and processing are simulated. It is determined whether surrounding blocks will be excavated or not. The blocks that can be extracted are also checked in terms of slope angle. Blocks that pass the test are connected to the branches. Due to the property inherent in dynamic programming, similar branches will be formed for each block. The biggest problem face with when using dynamic programming is that number of branches reaches to  $10^{100}$  in a short time. Thus,

forming branches should be restricted (Osanloo et al. 2008). Advantage of the method is that ultimate pit limit and production sequence are determined simultaneously. This approach is different compared to other production planning methods because unit cost is estimated in each iteration, and it includes the constraints for transportation, stocking, blending, and processing (Osanloo et al. 2008).

Parameterization is the mostly used method in long-term production planning. After the parameterization method introduced by Lerchs and Grossmann (1965), Matheron (1975) developed parametrical analysis in extraction sequence. The parameters in the optimization problem such as cost price and recovery are generally assumed to be constant. However, these parameters change with time. In parameterization, variables are not kept constant, they are systematically changed. By changing one (or two) parameter, a pit shape is generated. In this method, nested pits are formed. Nested pits are used for determining production sequence and ultimate pit limit. The purpose in parameterization is that variables that change with time are included in the production planning. The changes in pit size can be considered as sensitivity analysis (Özkan, 2015). Francois-Bongarcon and Marechal (1976), Francois-Bongarcon and Guibal (1984), Caccetta and Giannini (1988), Caccetta et al. (1998), Coléou (1988), Dagdelen and Johnson (1986), Whittle (1993) and Whittle (1998) conducted researches to apply and develop this method.

In addition to economic parameters, nested pits can be obtained by changing the grade of the blocks. Whittle (1993) uses economic block values to optimize production planning when creating nested pits. By increasing the price using a factor, nested pits are obtained. This factor is called as revenue adjustment factor. In general, increase in the size of the pits do not differ substantially. However, due to sudden changes in grade or irregularity in orebody results in huge differences between the nested pits, which is called as gap problem. In the end of the parameterization, different production rates are tested in determined limits. Advantages of this method are that it is easy to determine nested pits, only parameters are changed to find the limits, and sensitivity analysis can be made by changing price. Disadvantage of this method is that variables

such as time and production amount are indirectly included in the optimization model (Caccetta and Hill, 2003). It creates gap problem and it does not guarantee optimum solution. In addition, costs are assumed as constant. Moreover, operational constraints such as maximum depth and minimum width cannot be included in the model so extraction sequence is not compatible with operational requirements.

Some researchers applied reserve parameterization to production planning problem. The purpose in reserve parameterization is to determine the nested pits which give maximum metal content (Francois-Bongarcon and Guibal, 1982). This method of reserve parameterization is a complex problem to be solved (Özkan, 2015).

Lagrange relaxation is also used in production planning. Lagrange concept in mathematics is used, but it is mainly based on parameterization. In this method, complex problem with multiple periods is divided into single-period problems by using Lagrange multipliers. These single-periods can be solved with the algorithms used for determining ultimate pit limit. In Lagrange relaxation method, some constraints of the problem are multiplied with Lagrange multipliers and they are subtracted from the objective function (Held et al. (1974), Sandi (1979)). Then, Lagrange multipliers are arranged with sub-gradient method until optimum sequence is obtained. In every step, a problem similar to ultimate pit limit problem is solved. If there is no multiplier which leads to a solution for the constraints formed, this method does not give optimum solution. The disadvantage of this problem is that it does not include dynamic cutoff grade in the calculation. Akaike and Dagdelen (1999) proposed 4-Dimensional Lagrange relaxation approach and they included dynamic cutoff grade in this method.

Gershon (1987) developed a heuristic method for production planning since mathematical methods are complex and not practical, and conventional methods do not give optimum solutions. In this method, cones similar to the ones used in moving cone method are utilized. Difference from the moving cone method is that the cones are reversed. For each block inside the ultimate pit limit, an inverse cone is formed.

Value of the formed cones are assigned to the block. This value is called the positional weight. The block which has the highest positional weight is extracted first. Then, the positional weight of the blocks is calculated again. Gershon (1987) stated that if two blocks have similar positional weight, but they are on the different level, selection can be incorrect. Because of that, Gershon (1987) suggested that reduction factor should be used to avoid erroneous selection. In this way, blocks that are close to the surface will have higher positional weight.

Wang and Sevim (1992) attempted to improve positional weight method proposed by Gershon (1987) by determining ultimate pit limit and extraction sequence simultaneously and getting rid of gap problem in the parameterization methods. This method gives results close to the optimum solution. According to Wang and Sevim (1992), solution time of this method is lower than that of parameterization method. Although this technique has an advantage of finding ultimate pit limit and extraction sequence simultaneously, it is not guaranteed that the result is the optimum solution. Disadvantages of the moving cone method are also present in this method (Özkan, 2015). It is difficult to include other constraints since pit shapes are formed inversely (Thomas, 1996). Sevim and Lei (1994) used dynamic programming to obtain optimum sequence of nested pits obtained from the method proposed by Wang and Sevim (1992).

Aggregation is an approach in which the purpose is to decrease the size of the problem by converting the big data into small-sized clusters. This method is named as fundamental tree algorithm by Ramazan et al. (2005). In this method, linear programming is used, and blocks are gathered so that number of binary variables are decreased without deviating from the optimal solution. The blocks that are aggregated have a value greater than zero. They do not violate slope angle constraint, and they must not be divided into smaller group of blocks.

Kumral and Dowd (2004) used simulated annealing for production planning. In the proposed method, blocks having grade below cutoff grade are removed. Using one of

the optimization methods, a feasible (or an initial) solution is found for production planning in a short time. Then, using simulated annealing, sub-optimum solution is converted to nearly optimum or optimum solution.

Since genetic algorithm has some advantages to utilize, this metaheuristic method has been used in production scheduling by some researchers. Denby and Schofield (1994) used genetic algorithm to simultaneously determine production planning and ultimate pit limit. According to Osanloo et al. (2008), if variables in genetic algorithm are well defined, the method gives good results in a practical time period. Advantage of this method is that it simultaneously determines final limit and production planning. Disadvantage of this technique is that it can give different results for the same problem because it has stochastic features.

According to Albor Consuegra and Dimitrakopoulos (2010), pushbacks planned by using conventional methods bring on unmet production goals and predictions of net present value because uncertainty in variables are not incorporated in the optimization procedure. In their research, they used a stochastic integer programming to include uncertainty in pushback design. They state that the proposed technique results in approximately 30% increase in the net present value when the results are compared to the conventional methods. This increase is the result of different scheduling, rate of mining waste and extended pit contour.



## CHAPTER 3

### METHODOLOGY

#### 3.1. Basic Terminology for Surface Mining

The fundamental component of surface mining is the bench geometry. Basic terms used for the bench geometry are demonstrated in Figure 3.1. The range of bench face angle can be from  $55^\circ$  to  $80^\circ$  depending on rock properties. The proper choice of the bench face angle is essential because it can influence the overall slope angle (Hustrulid et al., 2016). The nomenclature can be defined as the following:

- Crest is the point where a bench face and top layer of the bench are intersected.
- Toe is the lowest point of the bench face.
- Overall slope angle is the angle between horizontal line and the line formed from the crest of the top bench to the toe of the bottom bench.
- Bench angle is the angle between the horizontal line and the line connecting the toe of the bench and the crest of the bench.

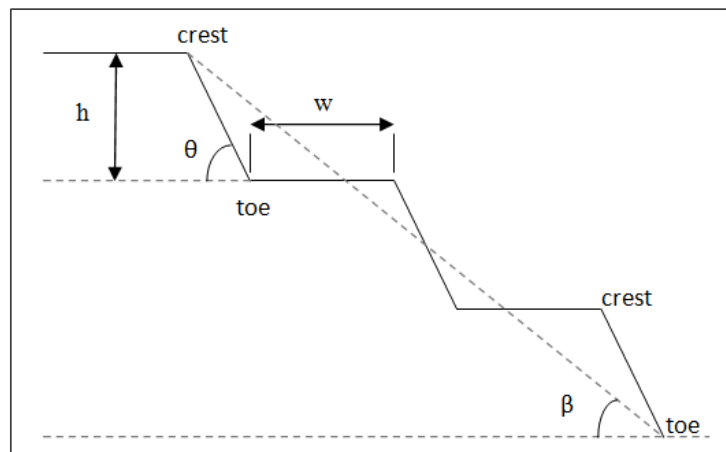


Figure 3.1. Bench geometry

where  $h$  is bench height,  $w$  is bench width,  $\beta$  is overall slope angle, and  $\theta$  is bench face angle.

### **3.2. Block Modeling and Economic Block Value**

Block modeling displays an orebody as a group of blocks to estimate grade and tonnage of the orebody. The size of the blocks is often chosen depending on bench height. Location of the blocks might be preferred based on the contact between orebody and overburden or between high grade and low-grade zones (Hustrulid et al., 2016). In block modeling, grade of the blocks is determined in the area where drill hole data is not available. After grade assignment, economic block values are calculated.

#### **3.2.1. Grade Assignment to Blocks**

There are certain techniques to estimate grades of blocks. The basic concept of these techniques is that grades of surrounding blocks in a certain area of a geometry have an effect on the grade of the block. The main difference in the grade estimation procedures is the means of choosing weighting coefficients which determine how much the grades of adjacent blocks affect the grade of the block under examination.

In this chapter, three approaches of grade estimation are explained:

- rule-of-nearest points,
- distance weighting technique,
- kriging.

In rule-of-nearest points approach, periphery of the area around the block center is formed in equal distances from closest points of known grade and the grade of the nearest block is assigned to the block. Only the grade of the closest point is considered in rule-of-nearest points method whereas the distance weighting technique includes

the influence of each surrounding grade point. Distance weighting approach can be applied with Equation 3.1. This technique is defined as the inverse distance weighting method.

$$g = \frac{\sum_{i=1}^n \frac{g_i}{d_i}}{\sum_{i=1}^n \frac{1}{d_i}} \quad (3.1)$$

The influence of grade decreases as the distance between the sample points increases. To include this property, the effect of distance can be intensified by increasing the power of  $d_i$  in Equation 3.1. If the power of  $d_i$  is 2, the equation turns out to be Equation 3.2. The general form is given by Equation 3.3. Equation 3.2 is the mostly used equation referred to as the inverse distance squared method. Equation 3.2 can be rewritten in a different version (Equation 3.4). The same formula as Equation 3.4 is used in the kriging method. The only difference is the way of finding the coefficients of the grades. Equation 3.4 is called linear estimator equation (Hustrulid et al., 2016).

$$g = \frac{\sum_{i=1}^n \frac{g_i}{d_i^2}}{\sum_{i=1}^n \frac{1}{d_i^2}} \quad (3.2)$$

$$g = \frac{\sum_{i=1}^n \frac{g_i}{d_i^m}}{\sum_{i=1}^n \frac{1}{d_i^m}} \quad (3.3)$$

$$g = a_1g_1 + a_2g_2 + \dots + a_n g_n \quad (3.4)$$

where  $g$  is the unknown grade,  $g_i$ 's are the known grades and  $a_i$ 's are weighting functions.

To apply kriging, and other distance weighting methods, it is necessary to determine the range of influence of a sample. Range of influence is the distance at which grade of sample points starts to be independent of each other. It is determined by a function showing the variance of grade with respect to distance between samples. The distances between sample pairs are called lag distances.

Basic steps to find range of influence are as follows:

- Pairs of grade points are placed in the same group if the lag distances are the same.
- The variance is calculated for each group using Equation 3.6. It is referred to as the semi-variance.
- Graph of variance versus lag distance is plotted. This plotted data is often represented by spherical (or Matheron) model to estimate the semi-variogram (Figure 3.2).

In the spherical model, grade variance attains a constant value as lag distance approaches to infinity. This constant value is called the sill. The spherical model is given by Equation 3.7. This model is also applied in different directions in order to check anisotropy in the orebody (Hustrulid et al., 2016).

When lag distance is zero, variance is expected to be zero. However, this is generally not the case because of inaccurate measurements or type of mineralization. Thus, in the plot, the part between the sill and the nugget effect is the correct depiction of the variance (Figure 3.2).

$$s^2(h) = \frac{1}{n(h)} \sum^n (g_i - g_j)^2 \quad (3.5)$$

$$\gamma(h) = \frac{1}{2n(h)} \sum^n (g_i - g_j)^2 \quad (3.6)$$

$$\gamma(h) = \begin{cases} c_1 \left( \frac{3h}{2a} - \frac{h^3}{2a^3} \right) + c_0 & \text{when } h \leq a \\ c_1 + c_0 & \text{when } h > a \end{cases} \quad (3.7)$$

Where  $c_1+c_0$  is the sill,  $h$  is the lag distance,  $a$  is the range of influence,  $c_0$  is the nugget effect.

In kriging, the semi-variogram is utilized to compute grade variance for several combinations of weighting coefficients. The best approximation of grade is obtained when minimum variance is achieved. The advantage of this approach is that both variance and grade is determined.

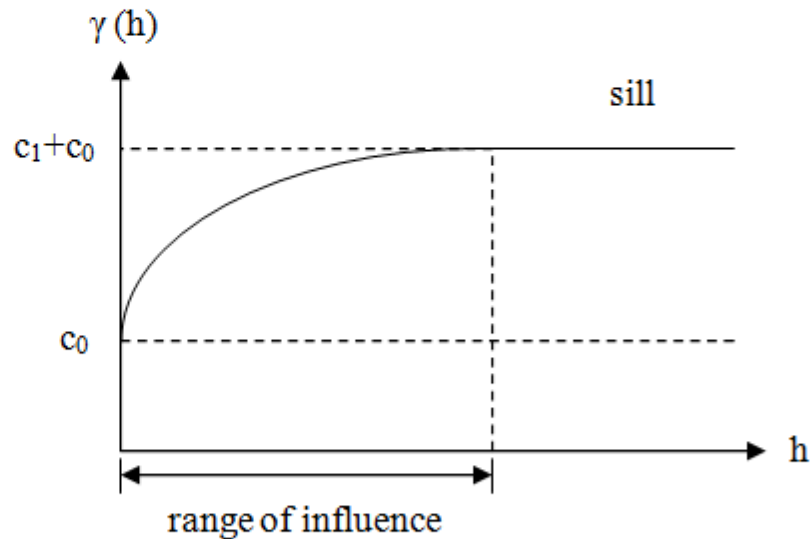


Figure 3.2. A spherical model of semi-variogram (Hustrulid et al., 2013)

### 3.2.2. Economic Block Value

To explain how economic value of a block is calculated, the following definitions are simply given:

- Revenue is the income obtained by selling the product.
- Mining cost is the cost resulted from extracting the product.
- Selling cost is the expense created to sell the product.

- Processing cost is the cost required to process the ore.
- Recovery is the percentage representing amount of ore recovered in mining or processing stage.

The equations to compute the value of a block are given as follows (Wiley, 2002):

$$R = (P - S) g t \quad (3.8)$$

$$EBV = \begin{cases} R - M_C t - P_C t & \text{for ore blocks} \\ -M_C t & \text{for waste blocks} \end{cases} \quad (3.9)$$

where R is revenue, P is price, S is selling cost, g is grade, t is tonnage of the block, EBV is economic block value,  $M_C$  is mining cost, and  $P_C$  is processing cost.

### 3.3. Geotechnical Slope Design

The main components considered in slope design for stability are overall slope angle which may change around the pit, slopes between the ramps, and the face angle and width of benches. Basic aspect of slope design methods is the shear force occurring between sliding faces. If shear force is greater than resisting force created by the shear strength of the rock, the slope is considered to be unstable. Some of the slope design methods are limit equilibrium approach, numerical analysis, and probabilistic approach (Wyllie & Mah, 2004).

#### 3.3.1. Limit Equilibrium Method

Limit equilibrium method is a conventional approach in stability assessment. In this method, factor of safety that is equal to total forces resisting instability divided by the total forces causing instability on the sliding plane is computed. If these forces are equivalent to each other, limiting equilibrium occurs and factor of safety is calculated as 1. Thus, this approach in stability assessment is called limit equilibrium method. Calculation of factor of safety differs depending on the type of failure such as plane, wedge, circular, and toppling failures. Value of factor of safety is mostly within the range of 1.2-1.4 (Wyllie & Mah, 2004).

### **3.3.2. Numerical Analysis**

Unlike in limit equilibrium method, factor of safety is determined by considering displacements rather than forces acting on sliding planes in numerical analysis. Mechanical effects of in-situ stresses, water levels, boundary conditions, and alterations due to excavation are determined in numerical analysis. Equilibrium or failure is the outcome of the numerical analysis. In this method, rock mass is divided into zones to which material model and properties are attributed. If the zones are disconnected, the model is called as discontinuum model; otherwise, it is called as continuum model.

In this analysis, factor of safety is calculated as the ratio of the shear strength to the minimum shear strength hindering collapse. Minimum shear strength is determined by reducing the shear strength until failure, which is called strength reduction (Wyllie & Mah, 2004).

### **3.3.3. Probabilistic Approach**

In deterministic approach, uncertainties in some values such as rock or joint properties, density, groundwater condition, and orientation of discontinuities are not taken into consideration. These uncertainties have an important effect on slope stability. Thus, probabilistic approaches are developed to evaluate these effects. The probability distribution of uncertain variables is used to determine probability of failure. Then, a method of probabilistic analyses such as Monte Carlo simulation, first-order second-moment method is applied (Khalokakaie, 1999).

## **3.4. Incorporation of Slope Design in Open Pit Optimization**

Incorporation of slope design into optimization process is carried out based on precedence relationship between the blocks. Methods determining precedence relationship between blocks can be classified as follows (Khalokakaie, 1999):

- Non-cone-based method
- Cone-based methods

In non-cone-based methods, a fixed block pattern is used. Some of the fixed block patterns can be seen in Figure 3.3. 1-5 (or 1-9) pattern indicates that five (or nine) overlying blocks must be removed to extract one underlying block.

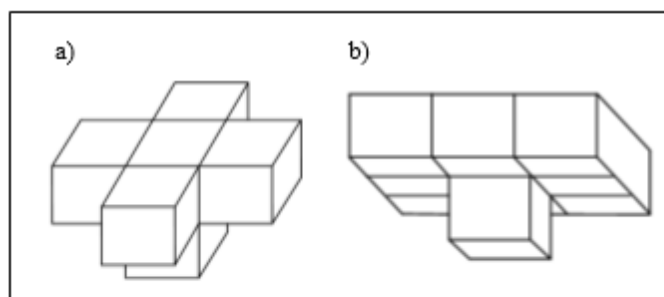


Figure 3.3. Precedence in extraction of blocks a) 1-5 Pattern b) 1-9 Pattern

According to Khalokakaie (1999), applying 1-5 block pattern produces  $45^\circ$  of overall slope angle and in some cross-sections, it produces  $55^\circ$  of overall slope angle. 1- 9 block pattern yields overall slope angle ranging from  $35^\circ$  to  $45^\circ$ . The main disadvantages of this method are that desired overall slope angle cannot be formed, and overall slope angle depends on block dimensions. Thus, utilizing cone-based methods is a suitable choice to obtain variable overall slope angles.

In cone-based methods, a cone is constructed in such a way that the apex of the cone is located on the base block and the blocks that are inside the cone are extracted. Using cone template, different overall slope angles can be included in the optimization process and slope angles can be independent of block dimensions. Generally, a cone smoothly tapers from a flat circular base to the apex. A cone with circular base can be used only for fixed overall slope angles with respect to azimuth. In order to implement different overall slope angles for different azimuths, cone base can be created by spline interpolation.

### 3.4.1. Spline Interpolation

Spline is a collection of  $k^{\text{th}}$  degree polynomials which are linked at given data points. Tangent vectors of the polynomials should be equal to each other at the given data points so that segments can be smoothly connected. In addition, derivatives of the polynomials must be equivalent to each other at the data points until their  $(k-1)^{\text{th}}$  derivative (Salomon, 2006).

According to Sattarvand & Shisvan (2012), spline interpolation is a more accurate method than linear interpolation for constructing cone templates (Figure 3.4). In addition, cubic spline interpolation creates more reasonable and smoother shapes compared to quadratic spline and cardinal spline interpolation (Figure 3.5). Thus, in the proposed method, cubic spline interpolation is chosen to be used.

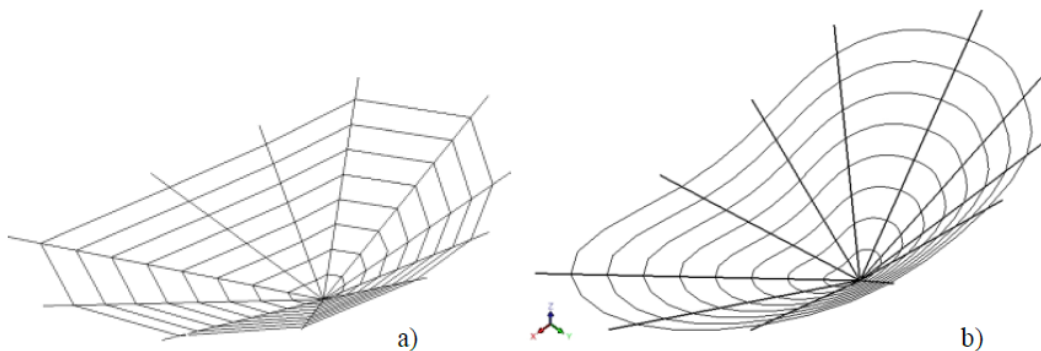


Figure 3.4. Shapes of cones formed by (a) linear and (b) spline interpolation (Sattarvand & Shisvan, 2012)

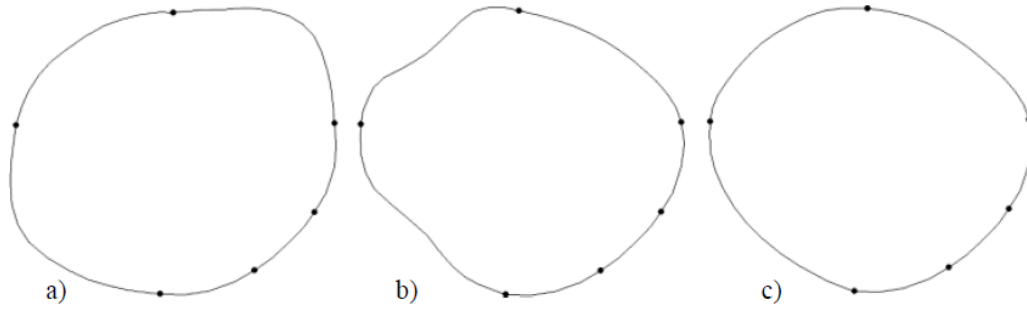


Figure 3.5. Shapes constructed with a) quadratic spline b) cardinal spline c) cubic spline (Sattarvand & Shisvan, 2012)

For cubic spline interpolation, the curve segments are represented by polynomial functions with parameter  $t$  (Equation 3.10). The first derivative of the function  $P(t)$  is denoted by  $P^t(t)$  (Equation 3.11). The coefficients ( $a$ ,  $b$ ,  $c$ , and  $d$ ) of the function are determined by using four equations. They are obtained from the equalities that are  $P(0) = P_k$ ,  $P(1) = P_{k+1}$ ,  $P^t(0) = P_k^t$  and  $P^t(1) = P_{k+1}^t$ . From those equalities, polynomial function with  $t$  is formed (Equation 3.12). It can be expressed in matrix form in Equation 3.13. In addition, the second derivatives of polynomial functions (Equation 3.12) should be the same at the given data point, i.e.,  $P_k^{tt}(1) = P_{k+1}^{tt}(0)$ . Applying that requirement, Equation 3.14 is derived, and its matrix form is given in Equation 3.15 (Salomon, 2006).

Equations 3.13 and 3.15 are used for the open pit optimization. These equations do not create closed curve. For example, for  $k$  number of points, the equations generate  $k-1$  number of curve segments. This problem can be solved by adding the first and second points again in the matrices (Sattarvand & Shisvan, 2012). The other solution can be redoing the calculation after changing the order of the points for one curve segment. The second approach is used in the proposed method.

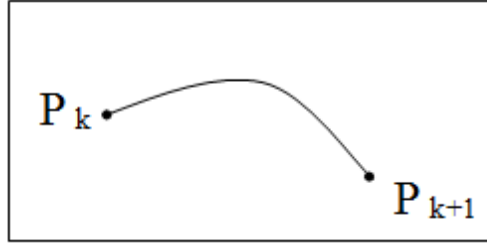


Figure 3.6. A segment of curve from point  $P_k$  to  $P_{k+1}$

$$P(t) = at^3 + bt^2 + ct + d \quad (3.10)$$

$$P^t(t) = 3at^2 + 2bt + c \quad (3.11)$$

$$P(t) = P_k + P_k^t \cdot t + (3(P_{k+1} - P_k) - 2P_k^t - P_{k+1}^t) \cdot t^2 + (2(P_k - P_{k+1}) + P_k^t + P_{k+1}^t) \cdot t^3 \quad (3.12)$$

$$P(t) = (t^3, t^2, t, 1) \begin{pmatrix} 2 & -2 & 1 & 1 \\ -3 & 3 & -2 & -1 \\ 0 & 0 & 1 & 0 \\ 1 & 0 & 0 & 0 \end{pmatrix} \begin{pmatrix} P_k \\ P_{k+1} \\ P_k^t \\ P_{k+1}^t \end{pmatrix} \quad (3.13)$$

$$P_k^t + 4P_{k+1}^t + P_{k+2}^t = 3(P_{k+2} - P_k) \quad (3.14)$$

$$\begin{bmatrix} 1 & 4 & 1 & \dots & 0 & \dots & 0 \\ 0 & 1 & 4 & 1 & \dots & \dots & 0 \\ & & & \ddots & \ddots & & \vdots \\ 0 & \dots & \dots & \dots & 1 & 4 & 1 \\ 1 & \dots & \dots & \dots & 0 & 1 & 4 \\ 4 & 1 & 0 & \dots & 0 & 0 & 1 \end{bmatrix}_{(n \times n)} \begin{bmatrix} P_1^t \\ P_2^t \\ P_3^t \\ \vdots \\ P_{n-1}^t \\ P_n^t \end{bmatrix} = \begin{bmatrix} 3(P_3 - P_1) \\ 3(P_4 - P_2) \\ \vdots \\ 3(P_{n+1} - P_{n-1}) \\ 3(P_{n+2} - P_n) \end{bmatrix} \quad (3.15)$$

### 3.4.2. Application of Cubic Spline Interpolation for Variable Overall Slope Angles

Cubic spline interpolation enables any number of different overall slope angles to be attained at any azimuth. The steps of cubic spline interpolation for variable overall slope angles are as following (Sattarvand & Shisvan, 2012):

- Slope and azimuth angles are converted into points of x and y coordinates by using Equations 3.16-3.19. The equations are obtained by geometrical relationships demonstrated in Figure 3.7.
- Polynomial functions of variable t are created for both x and y coordinates with points obtained in the previous step. By substituting x and y coordinates into the right-hand side of Equation 3.15,  $P_k^t$  values are found for x and y separately. Then,  $P_k^t$  values are substituted into Equation 3.12. For k points given, (k-1) number of polynomial functions for x and (k-1) number of polynomial functions for y are obtained.
- Values in the range of 0 and 1 are given to parameter t for all polynomial functions in order to determine a set of points on the curve segment,
- Cubic spline interpolation is performed for each level. In this way, cone template is constructed.

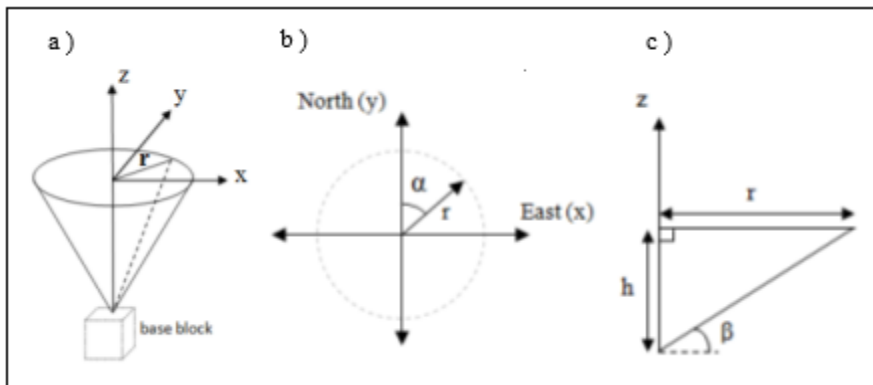


Figure 3.7. Cone template's a) isometric, b) top, and c) side view

$$r = \frac{h}{\tan \beta} \quad (3.16)$$

$$x^2 = r^2 - y^2 \quad (3.17)$$

$$y = x \cot \alpha \quad (3.18)$$

$$x = \pm \frac{h}{\tan \beta \sqrt{1 + \cot^2 \alpha}} \quad (3.19)$$

where  $h$  is depth,  $\alpha$  is azimuth,  $\beta$  is overall slope angle, and  $r$  is radius of the cone.

To explain cubic spline interpolation further, an example that consists of 4 different overall slope angles is presented. The overall slope angles and azimuths are given in the Table 3.1. For  $h=10$  m, the corresponding  $x$  and  $y$  coordinates of the points are determined by using Equations 3.16-3.19. The points are provided in the Table 3.2. Then, they are inserted in Equation 3.20 to obtain the  $P_k^t$  values. The  $P_k^t$  values and the points in the Table 3.2 are substituted in Equations 3.23-3.25, which results in six polynomial functions for  $x$  and  $y$  coordinates. Giving values from 0 to 1 to parameter  $t$  in the polynomial functions, the curve is formed. The curve can be seen in Figure 3.8. If interpolation is executed for five levels, i.e., from 10 m to 50 m of height, the cone shape in Figure 3.9 is obtained.

Table 3.1. Different overall slope angles for different azimuths

Angle	Point 1	Point 2	Point 3	Point 4
Azimuth	45°	120°	210°	330°
Overall Slope Angle	30°	35°	45°	36°

Table 3.2. Corresponding  $x$  and  $y$  coordinates of the points given in the Table 3.1

Coordinates	Point 1	Point 2	Point 3	Point 4
$x$	12.25	12.37	-5	-6.88
$y$	12.25	-7.14	-8.66	11.92

$$\begin{bmatrix} P_1^t \\ P_2^t \\ P_3^t \\ P_4^t \end{bmatrix} = \begin{bmatrix} 1 & 4 & 1 & 0 \\ 0 & 1 & 4 & 1 \\ 1 & 0 & 1 & 4 \\ 4 & 1 & 0 & 1 \end{bmatrix}^{-1} \begin{bmatrix} 3(P_3 - P_1) \\ 3(P_4 - P_2) \\ 3(P_1 - P_3) \\ 3(P_2 - P_4) \end{bmatrix} \quad (3.20)$$

$$\begin{bmatrix} P_1^t(x) \\ P_2^t(x) \\ P_3^t(x) \\ P_4^t(x) \end{bmatrix} = \begin{bmatrix} 14.4 \\ -12.9 \\ -14.4 \\ 12.9 \end{bmatrix} \quad (3.21)$$

$$\begin{bmatrix} P_1^t(y) \\ P_2^t(y) \\ P_3^t(y) \\ P_4^t(y) \end{bmatrix} = \begin{bmatrix} -14.3 \\ -12.9 \\ 14.3 \\ 12.9 \end{bmatrix} \quad (3.22)$$

$$P_1(x \text{ or } y) = P_1 + P_1^t \cdot t + (3(P_2 - P_1) - 2P_1^t - P_2^t) \cdot t^2 + (2(P_1 - P_2) + P_1^t + P_2^t) \cdot t^3 \quad (3.23)$$

$$P_2(x \text{ or } y) = P_2 + P_2^t \cdot t + (3(P_3 - P_2) - 2P_2^t - P_3^t) \cdot t^2 + (2(P_2 - P_3) + P_2^t + P_3^t) \cdot t^3 \quad (3.24)$$

$$P_3(x \text{ or } y) = P_3 + P_3^t \cdot t + (3(P_4 - P_3) - 2P_3^t - P_4^t) \cdot t^2 + (2(P_3 - P_4) + P_3^t + P_4^t) \cdot t^3 \quad (3.25)$$

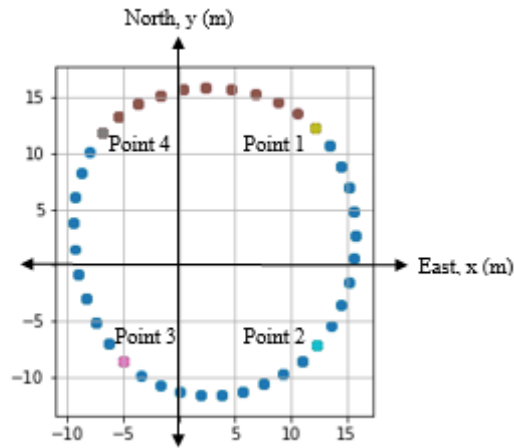


Figure 3.8. Points created by spline interpolation in plan view

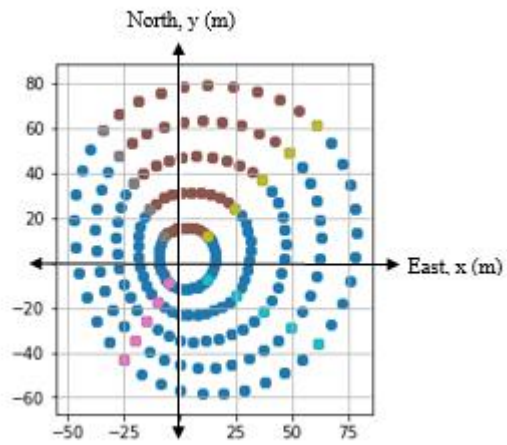


Figure 3.9. Five levels of points created by spline interpolation in plan view



## CHAPTER 4

### ALGORITHM DEVELOPMENT

The algorithm was created so that maximum profit can be found while attaining required overall slope angle. The solution obtained from the algorithm gives depth of pit, maximum radius of the pit, bench width, and total economic value of blocks.

In the algorithm, firstly, maximum number of benches is determined. Then, for a certain number of benches, the mathematical model is generated, and integer values are assigned to variable nb (number of benches) and for each value, optimization is carried out. Then, nb which gives the maximum result is selected. A simple version of the algorithm is provided as a pseudo-code in Figure 4.1. The pseudocode of the spline interpolation in the algorithm are given in Appendix A.

For each nb, a cone template is formed by using spline interpolation if multiple overall slope angles are required to be included in the problem. If the angle is constant, a circular cone base is used. In the optimization process, cone size changes depending on economic block values. If the block is inside the cone, then it is considered as selected or extracted.

The algorithm was written in Python Programming Language which is an object-oriented, general-purpose programming language. It provides many modules and packages. The following modules, packages, and libraries were used in the code:

- PuLP
- NumPy
- Math
- Pandas
- Matplotlib

- Tkinter

PuLP is a module written in Python Programming Language for optimization purposes. It creates the model of a problem and calls solvers (“PuLP 1.6.10”, n. d.). With PuLP module, mathematical model is formed, and optimization is performed. In this code, the mixed integer programming solver was used.

NumPy is a package used for scientific calculations in Python. It includes functions such as n-dimensional array and linear algebra functions (“NumPy”, n. d.). In the code, the functions for matrix calculations were used.

Math module contains basic mathematical functions (“Math-Mathematical functions”, n. d.). In the code, trigonometric, power, square root functions were utilized.

Pandas is a library written for data analysis. It offers tools for reading and writing CSV and text files, Microsoft Excel, SQL databases, and the HDF5 format (“Python Data Analysis Library”, n. d.). It was used for reading and writing Microsoft Excel files of the block data in the code.

Matplotlib is a 2D plotting library in Python Programming Language (“Matplotlib”, n. d.). It was used for generating 2D figures in the code. Mplot3d which is one of the toolkits in Matplotlib library was used for obtaining 3D figures in the code.

Tkinter is a tool for creating graphical user interface. Tkinter includes widgets such as entry boxes, buttons, message boxes, check buttons for entering input data and displaying output data (“Graphical User Interfaces with Tk”, n. d.).

```

Input: Parameters used for calculating economic block value
         Bench parameters
         Overall slope change pattern
Determine the depth of the block model
Calculate  $m = \text{depth/bench height}$ 
From  $n=1$  to  $n=m$ :
         If overall slope angle changes with respect to azimuth:
             Call the function of cubic spline interpolation
         Generate MIP mathematical model
         Find solution for  $n$ 
Determine the value of  $n$  which gives the maximum value of the objective function
Output: The maximum radius and the depth of the final pit limit
         Extracted blocks
         Non-extracted blocks
         Total economic block value

```

Figure 4.1. Pseudo-code for the main steps of the algorithm

#### 4.1. Incorporation of Overall Slope Angles in the Model

The incorporation of required overall slope angles is based on constant or various values of bench width that are used in the model. Bench width is kept constant if overall slope angle is kept constant throughout the orebody. However, bench width is changed if different overall slope angles are required to be incorporated in the design. After determining different angles that are generated by spline interpolation, bench width is calculated by utilizing Equation 4.1. Then, positions of the blocks are converted into radii and values of bench width are inserted in Equation 4.2. Radius of the pit on the level where the block is located and radius of the block are calculated

by Equation 4.2 and Equation 4.3, respectively. Then, R and r are used to express the following condition:

*Condition:* If R is greater than or equal to r, the block is included in the pit, i.e. the block is extracted (Figure 4.2 and 4.3).

The center of the blocks is considered when checking whether this condition is satisfied or not.

$$W = \frac{nb h (\tan \theta - \tan \beta)}{(nb - 1) \tan \theta \tan \beta} \quad (4.1)$$

$$R = L - \frac{z}{\tan(\theta)} - w (bl - 1) \quad (4.2)$$

$$r = \sqrt{x^2 + y^2} \quad (4.3)$$

where

w bench width

nb number of benches

$\theta$  bench slope angle

$\beta$  overall slope angle

R the distance between the boundary of the pit and the center of pit

r the distance between the block and the center of the pit

L maximum radius of the ultimate pit

bl bench level on which the block is located

z depth of the block

x perpendicular distance from the center of the block to the y-axis



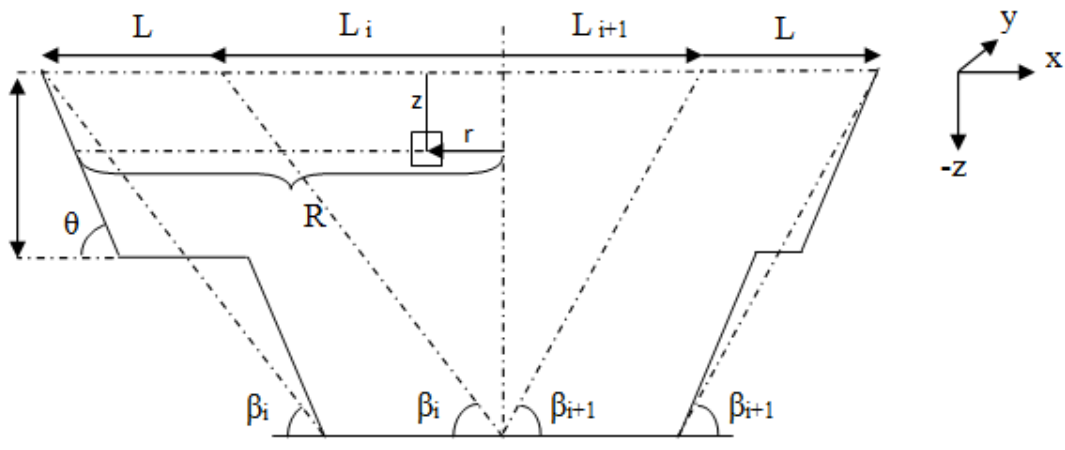


Figure 4.4. Different overall slope angles in different azimuth directions

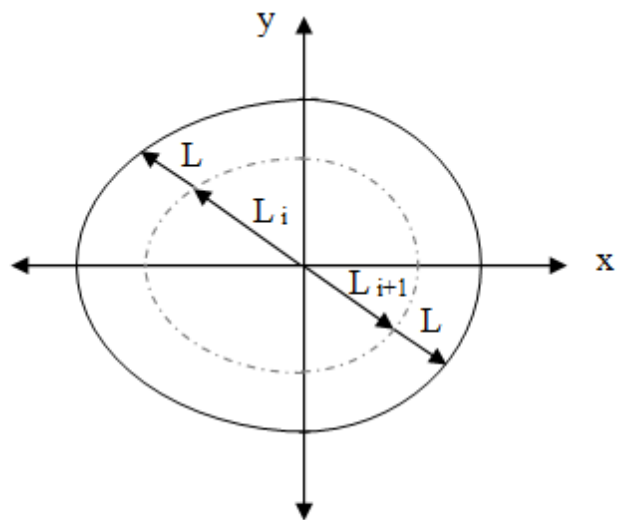


Figure 4.5. Plan view of the pit shape in Figure 4.4

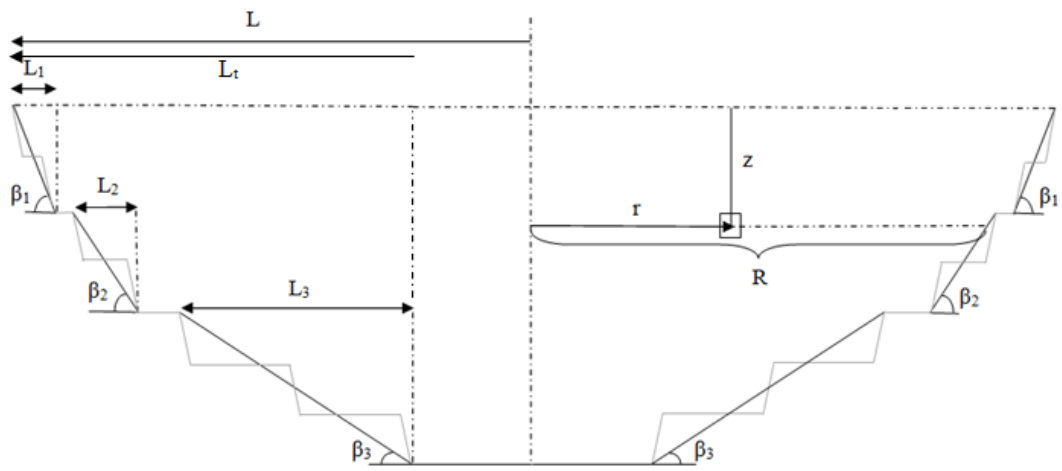


Figure 4.6. Different overall slope angles in different depth ranges

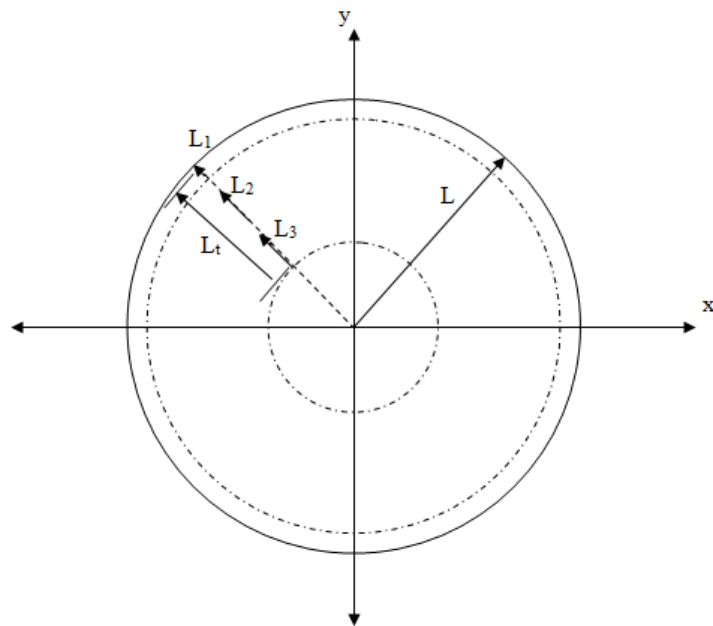


Figure 4.7. Plan view of the pit shape given in Figure 4.6

## 4.2. Mixed Integer Programming

Mixed integer programming is applied in the algorithm since there are binary and continuous decision variables in the problem. The objective function consists of economic block values and binary values of the blocks (Equation 4.4). Constraints provide results in accordance with overall slope angles and ensure restriction on maximum and minimum magnitude of pit radius (Equation 4.5-4.9). Optimal solution gives values of binary blocks and maximum radius of the pit.

In the defined set of constraints given in Equation 4.7 and 4.8, any constant number large enough to produce an optimum result can be used for  $M$ . These equations are created to implement the following condition in the model:

*Condition 1:* If block  $b_i$  is included in the pit,  $R_i - r_i$  must be greater than or equal to 0 and  $b_i$  is 1.

*Condition 2:* If block  $b_i$  is not included in the pit,  $R_i - r_i$  must be less than 0 and  $b_i$  is 0.

$$\text{Maximize } \sum_{i \in I} EBV_i b_i \quad (4.4)$$

Subject to

$$L \leq \max(r) + \frac{nb h}{\tan(\beta)} \quad (4.5)$$

$$L \geq \frac{nb h}{\tan(\beta)} \quad (4.6)$$

$$R_i - r_i \geq -M (1 - b_i) \quad (4.7)$$

$$R_i - r_i < M b_i \quad (4.8)$$

$$b_i \in \{0, 1\}, \quad \forall i \in I; \quad (4.9)$$

where

EBV <sub>i</sub>	economic block value
x <sub>n</sub>	total number of blocks in x-direction
y <sub>n</sub>	total number of blocks in y-direction
dx	block dimension in x-direction
dy	block dimension in y-direction
i	block
I	set of all blocks
b <sub>i</sub>	binary decision variable that is equal to 1 if the block i is mined
M	a large constant
max(r)	maximum of radii of blocks

The main objective function used for constant overall slope angle is given in Equations 4.4-4.9.  $R_i$  equation depends on the location of the block and variation of overall slope angle. If the overall slope angle changes as the azimuth varies, L constraint and  $R_i$  equation turn into Equations 4.10 and 4.11. If overall slope angle changes in the different ranges of depth, L constraint turns into Equation 4.12 and in this case, if the depth range in the upper levels is equal to or less than bench height,  $R_i$  is calculated as in Equation 4.13. If there are different magnitudes of bench width in the depth ranges in one of the levels, they are also subtracted from Equation 4.2. For example, the equation used for the pit shape given in Figure 4.6, 4.8, and 4.9 are formed as Equation 4.13, 4.14, and 4.15. If the overall slope angle changes with respect to both azimuth and depth, to calculate  $R_i$ , equations of  $R_i$  in the cases where overall slope changes with respect to depth and azimuth are combined. The constraint for L is expressed as in Equation 4.10.  $L_i$  is added to Equation 4.14.

$$0 \leq L \leq \max(r) \quad (4.10)$$

$$R_i = L + L_i - \frac{z}{\tan(\theta)} - w (bl - 1) \quad (4.11)$$

where  $L_i$  is equal to  $(nb \times h)/\tan(\beta_i)$  and  $\beta_i$  is  $i^{\text{th}}$  overall slope angle

$$L_t \leq L \leq \max(r) + L_t \quad (4.12)$$

$$R_i = L - \frac{z}{\tan\theta} - 1 \times w_1 - 0 \times w_2 - L_1 \quad (4.13)$$

$$R_i = L - \frac{z}{\tan\theta_1} - 1 \times w_1 - 1 \times w_2 - L_1 \quad (4.14)$$

$$R_i = L - \frac{z - L_1 \times \tan\beta_1}{\tan\theta_2} - 1 \times w_1 - 0 \times w_2 - L_1 \quad (4.15)$$

where  $w_1$  and  $w_2$  are the bench widths in the depth range 1, and the depth range 2, respectively

$$w_1 = \frac{n_1 h (\tan\theta - \tan\beta_1)}{(n_1 - 1)\tan\theta \tan\beta_1} \quad (4.16)$$

$$w_2 = \frac{n_2 h (\tan\theta - \tan\beta_2)}{(n_2 - 1)\tan\theta \tan\beta_2} \quad (4.17)$$

where  $n_1$  and  $n_2$  are number of benches in a depth range

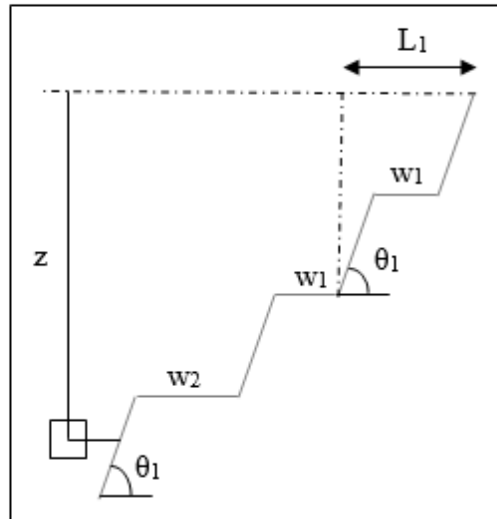


Figure 4.8. A section of a pit

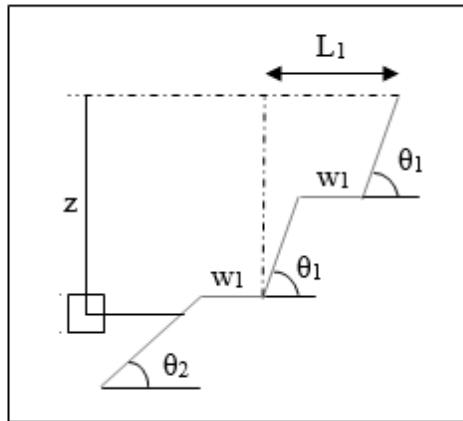


Figure 4.9. A section of a pit with different slope angle

### 4.3. Verification of the Algorithm

In this part, hypothetical block models are used to verify the mathematical model and the algorithm. For this purpose, one example with small number of blocks, and four examples with larger number of blocks are given, and overall slope angles are checked whether required angles are obtained or not.

The example in Figure 4.10 is given for demonstrating the case of constant overall slope angle. In this example, number of blocks is 4913, block dimensions are equal, and the overall slope angle is aimed to be  $45^\circ$ . A cross-sectional view is taken from the result produced by the algorithm (Figure 4.10). In cross section AA, overall slope angle is measured as  $45^\circ$  (Figure 4.11).

In some cases, required angle may not be acquired but an approximate value is obtained because a block is extracted if its center is in the cone template even if the whole block is not inside the cone template. Selected and unselected blocks in this manner and cone template are illustrated in Figure 4.12 and 4.13.

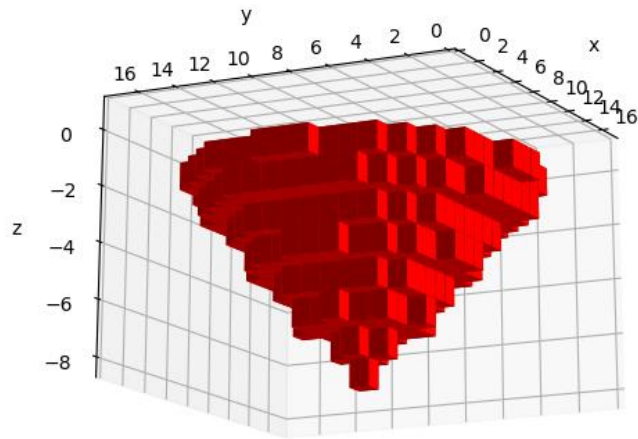


Figure 4.10. Extracted blocks with 45° overall slope

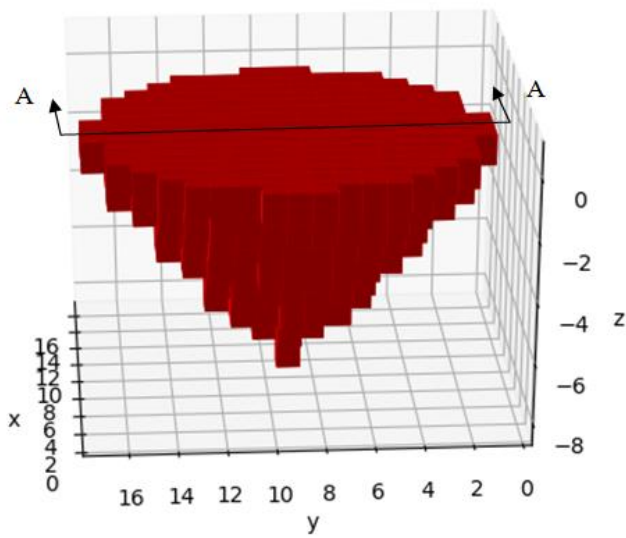


Figure 4.11. Section view of the block model

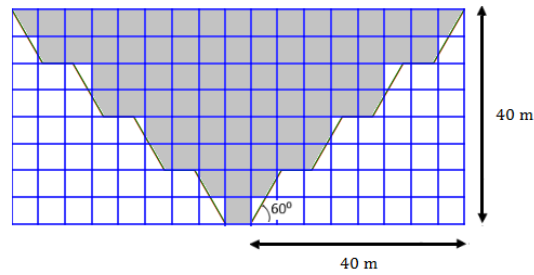


Figure 4.12. Cross-section "A-A"

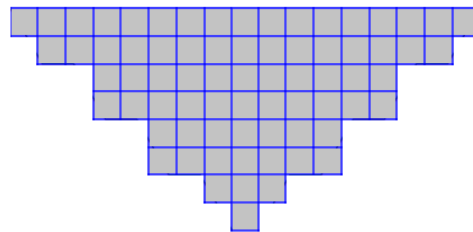


Figure 4.13. Selected blocks

To validate the algorithm, four examples with larger number of blocks are also given. Bench height and bench face angle are given in Table 4.1 and these values are used for all four examples. Number of blocks can be viewed in Table 4.3. The first example is provided for constant overall slope angle and the angle is  $51^{\circ}$ . The second example is presented to check the algorithm for overall slope change with respect to azimuth. The third example is provided for the cases in which overall slope angle varies with respect to depth. The fourth example is given for change in overall slope angle with respect to depth and azimuth. The fourth example is also used for demonstrating an example for lignite deposit. For lignite, only calculation of economic block value is different in the code because calorie is used instead of grade in calculations. As it can be seen from the results of the examples presented (Table 4.4, 4.6, 4.8 and 4.10), it can be stated that algorithm can produce reasonable solutions.

Table 4.1. Input values

<b>Bench face angle</b>	60
<b>Bench height</b>	10

Table 4.2. Block dimensions

<b>Block dimensions</b>	
dx	10
dy	10
dz	2

Table 4.3. Number of blocks

<b>Number of blocks</b>	
Example 1	86,100
Example 2	86,100
Example 3	107,916
Example 4	118,096

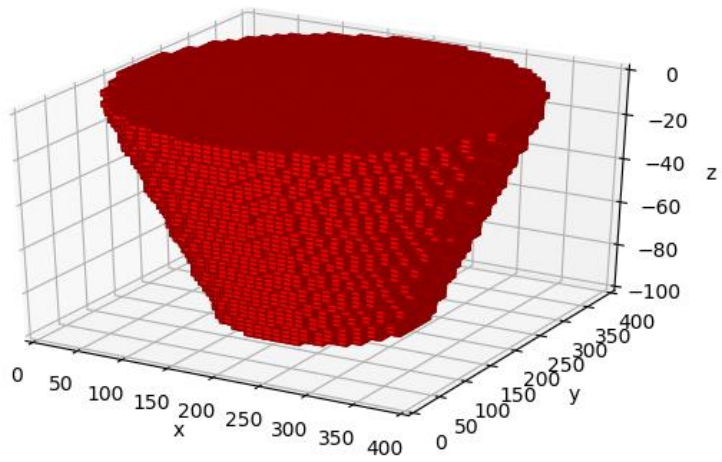


Figure 4.14. Constant overall slope angle

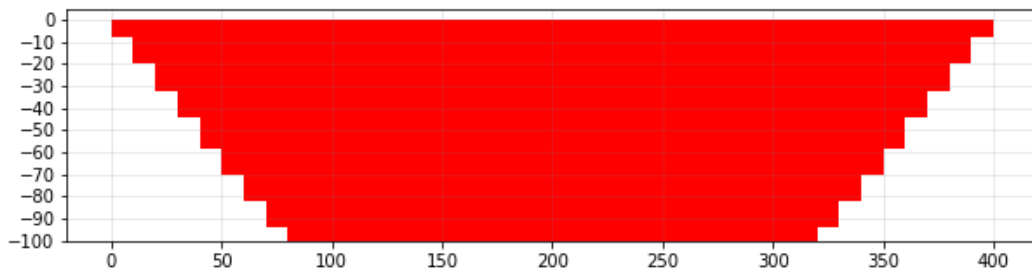


Figure 4.15. W-E section of the extracted blocks for the first example

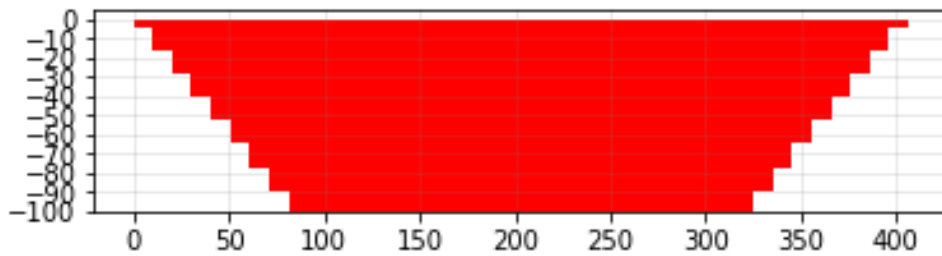


Figure 4.16. N 10 E section of the extracted blocks for the first example

Table 4.4. Comparison of overall slope angles for the first example

<b>Overall slope angle</b>		
<b>Cross-sections</b>	<b>Input value</b>	<b>Measured value</b>
N10E	50	50.912
W-E	50	51.340

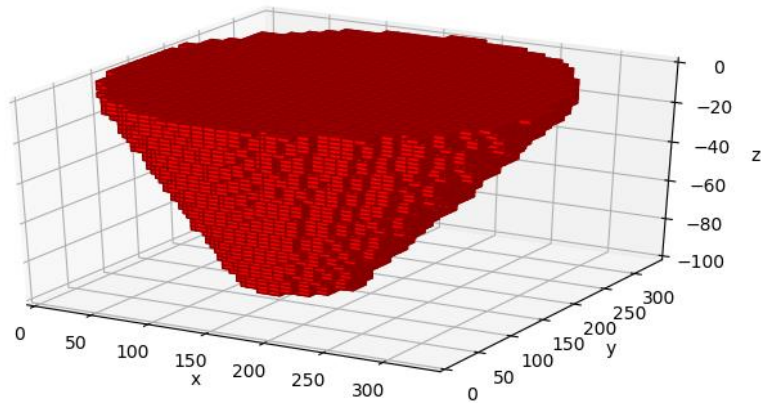


Figure 4.17. Extracted blocks of the second example

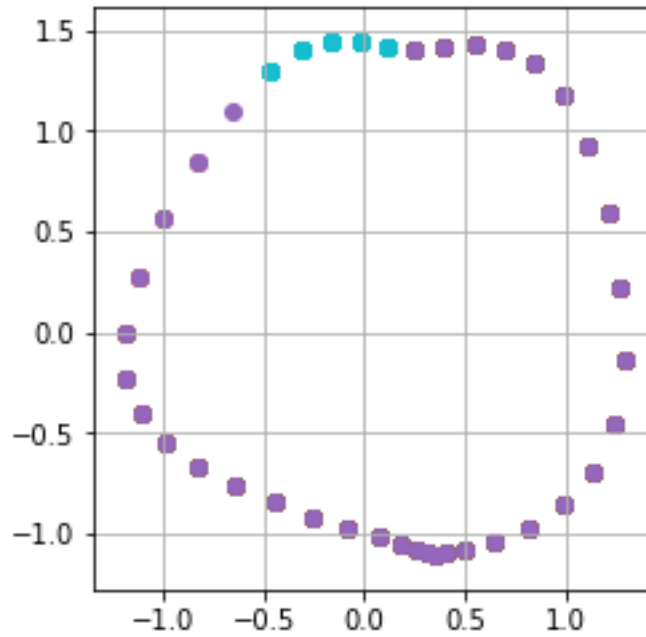


Figure 4.18. Curve created by using spline interpolation for the second example

Table 4.5. Overall slope angle inputs for the second example

Overall slope angle	Azimuth (from)	Azimuth (to)
35	0	20
33	35	45
37	100	120
40	150	160
43	160	180
45	215	225
40	265	285
36	330	350

Table 4.6. Comparison of overall slope angles for the second example

Overall slope angle				
Cross sections	Input value	Measured value	Input value	Measured value
N 40 E	45	44.757	33	32.553
S 30 W	36	35.538	40	39.806

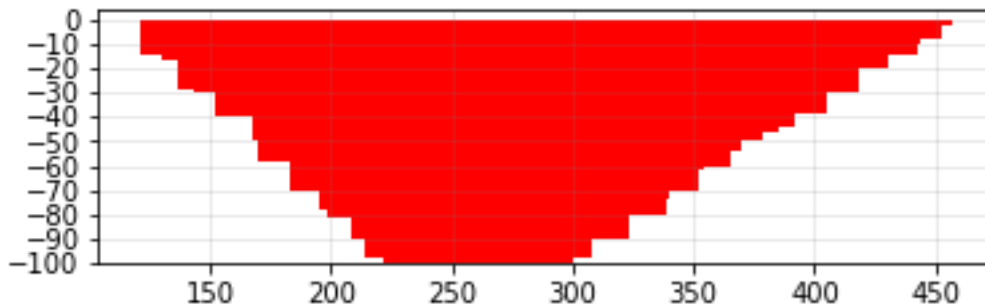


Figure 4.19. N 40 E section of the extracted blocks for the second example

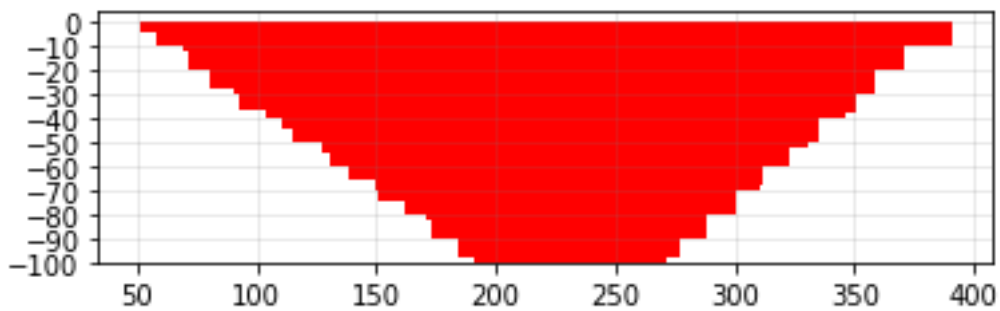


Figure 4.20. S 30 W section of the extracted blocks for the second example

Table 4.7. Input values for the third example

<b>Overall slope angle</b>	<b>Depth (from)</b>	<b>Depth (to)</b>
45	0	50
20	50	100

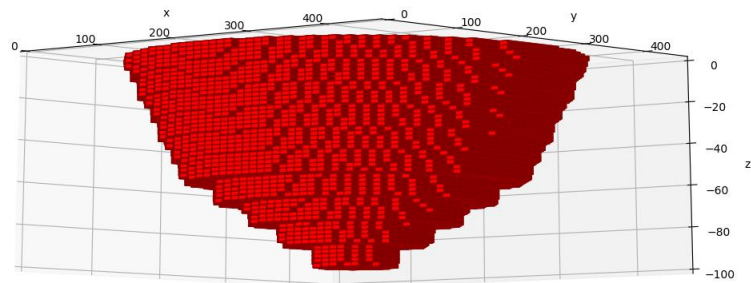


Figure 4.21. Extracted blocks of the third example

Table 4.8. Comparison of overall slope angles for the third example

<b>Cross-sections</b>	<b>Overall slope angle</b>			
	<b>Input value</b>	<b>Measured value</b>	<b>Input value</b>	<b>Measured value</b>
<b>N40E</b>	45	44.657	20	20.751
<b>W-E</b>	45	45	20	21.038

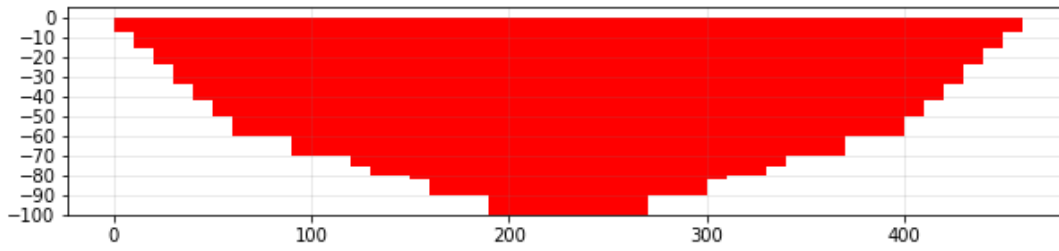


Figure 4.22. W-E section of the extracted blocks for the third example

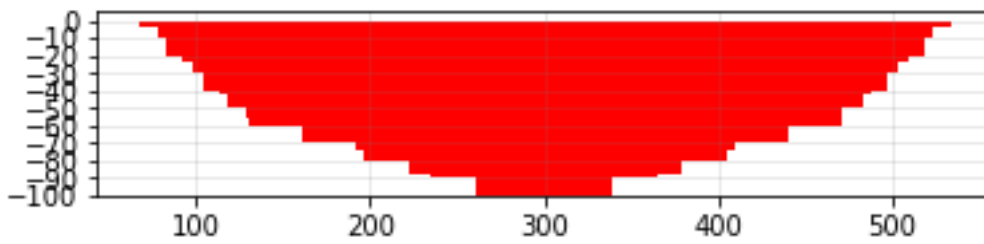


Figure 4.23. N 40 E section of the extracted blocks for the third example

Table 4.9. Overall slope angles for the fourth example

<b>Depth range</b>	<b>Overall slope angle</b>	<b>Azimuth (from)</b>	<b>Azimuth (to)</b>
0-60	42	0	90
	40	90	180
	43	180	270
	45	270	360
60-120	38	0	90
	36	90	180
	39	180	270
	41	270	360

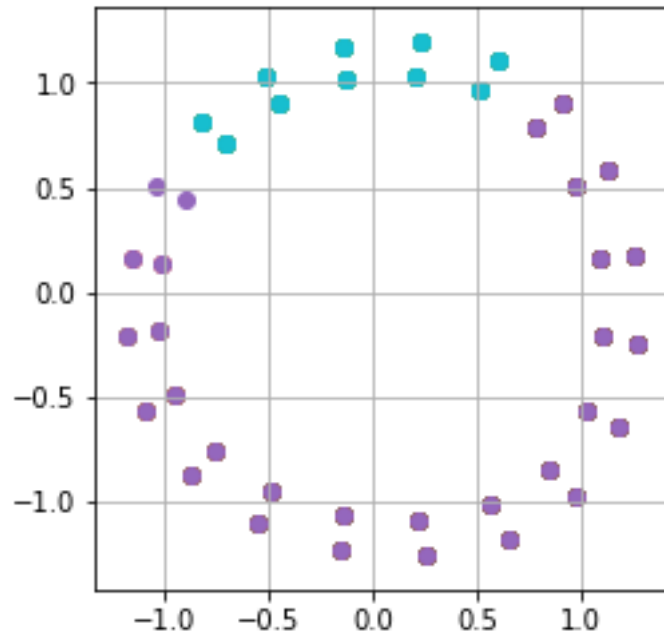


Figure 4.24. Curve created by using spline interpolation for the fourth example

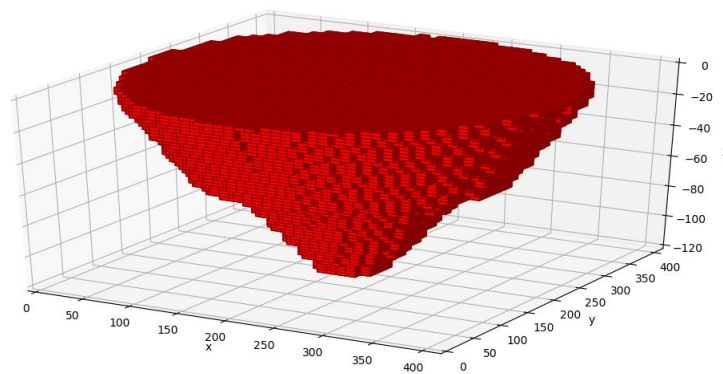


Figure 4.25. Extracted blocks of the fourth example (lignite deposit)

Table 4.10. Comparison of overall slope angles for the fourth example

<b>Overall slope angle</b>					
<b>Cross-sections</b>	<b>Depth range</b>	<b>Input value</b>	<b>Measured value</b>	<b>Input value</b>	<b>Measured value</b>
<b>N 45 E</b>	1	43	35.264	42	40.316
	2	39	40.315	38	35.264
<b>S 45 E</b>	1	45	46.686	40	40.315
	2	41	40.315	36	35.264

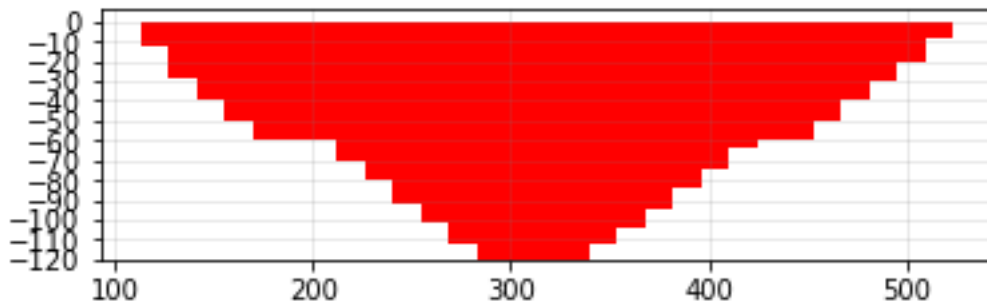


Figure 4.26. N 45 E section of the extracted blocks for the fourth example

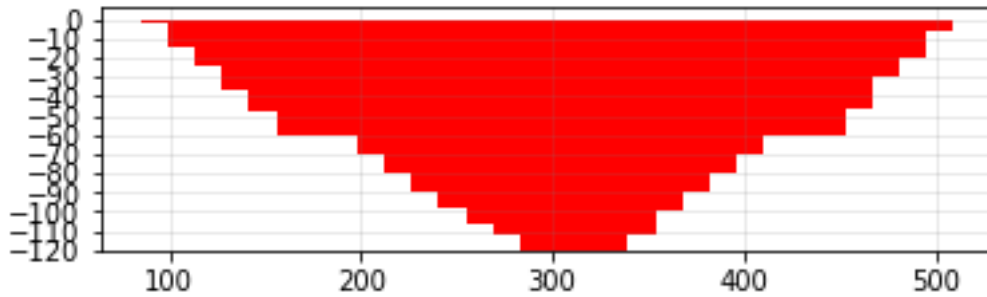


Figure 4.27. S 45 E section of the extracted blocks for the fourth example

It should be noted that the generated pit shape by the code becomes more similar to the required pit shape as the number of blocks increases or block dimensions decreases. To demonstrate that, second example is compared to another example with the same input but larger number of blocks. The number of blocks of the large block model is 494,900. The difference between input and output values is smaller in large block models. This is demonstrated in Figure 4.28. Its output value is closer to the value produced by the interpolation. The overall slope angles and the differences are given in Appendix C.

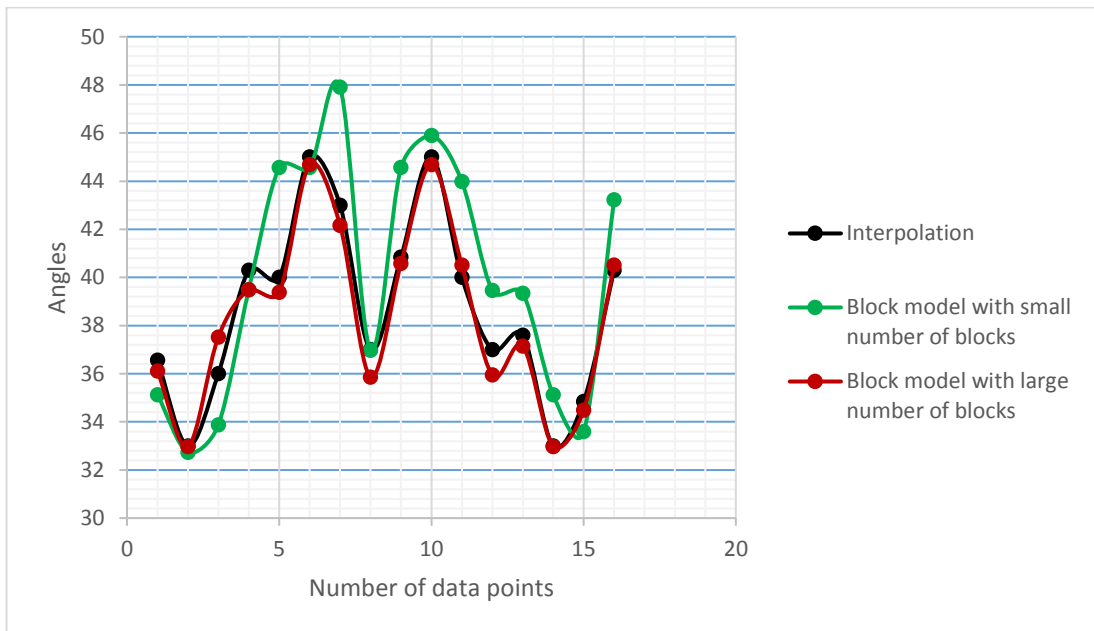


Figure 4.28. Comparison between input and output values of overall slope angles of the block models with large and small number of blocks



## CHAPTER 5

### THE GRAPHICAL USER INTERFACE

The coding was performed in the Python Programming Language and Tkinter toolkit was used to construct the user interface. With this interface, mainly two parts are developed for input data and output data. In the Graphical User Interface (GUI) created for input data, the parameters used for the calculation of economic block value and the parameters used for the pit geometry are entered to determine optimum pit limit. In the windows for output data, the results of optimization are provided by figures and the extracted and non-extracted blocks are saved in separate MS Excel files.

#### 5.1. GUI for Input Data

The data entry windows vary based on the number of overall slope angle required. In the first window that appears when the code is run, the input data required to be entered is the economic block value parameters and bench parameters. A selection must be also made for overall slope change pattern (Figure 5.1). In the first pane of the window, required parameters are price, selling cost, mining cost, and processing cost. Costs are given per tonne of ore. Average density is used to find the tonnage of a block and its unit is tonne/m<sup>3</sup> (or g/cm<sup>3</sup>). Mining cost increases per meter of depth and can be 0 or greater than 0. Recovery is given in percentage. With these parameters, Equations 3.8 and 3.9 are used to calculate the economic block value. In the second pane, bench height (m) and bench face angle are entered. When entering the parameters, any unit can be used as long as their units are consistent with each other. In the third pane, cases for overall slope change pattern are provided. One of the cases must be chosen. In the fourth pane, if 3D figures of extracted and/or non-extracted blocks need to be displayed, one or two displaying choices can be selected.

Figure 5.1. Entry window for data input

The four cases one of which must be selected are as follows:

- Case 1: Constant overall slope angle.
- Case 2: Overall slope angle change with respect to azimuth.
- Case 3: Overall slope angle change with respect to depth.
- Case 4: Overall slope angle change with respect to depth and azimuth.

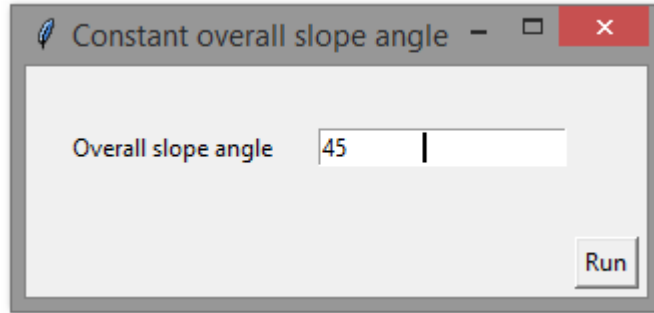


Figure 5.2. Case 1: Entry window for overall slope angle

In case 1, the overall slope angle is the same throughout the orebody. For this reason, spline interpolation is not used. If case 1 is chosen, the second window that appears is given in Figure 5.2. In this window, overall slope angle is entered. The angle can be between  $0^\circ$  and the bench slope angle entered in the first window due to geometrical limits.

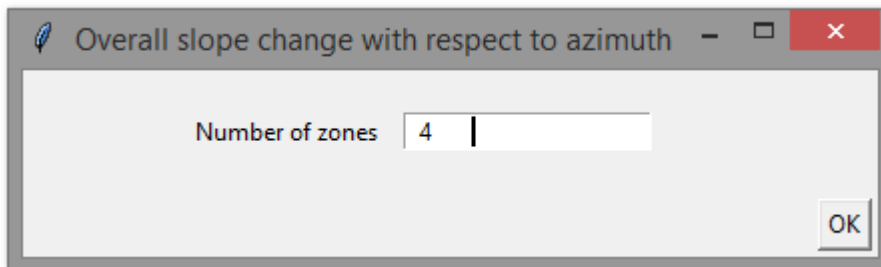


Figure 5.3. Case 2: Entry window for number of zones

	Overall slope angle	(from) Azimuth	(to) Azimuth
Zone 1	30	40	90
Zone 2	45	120	160
Zone 3	40	190	240
Zone 4	35	290	350

Figure 5.4. Case 2: Entry window for overall slope angles in different azimuth ranges

In case 2, the overall slope angle is not invariable for different azimuth ranges. Thus, spline interpolation is used in this case. The second window that shows up if this case is selected can be seen in Figure 5.3. Number of different overall slope angles are entered in this window. Any integer number greater than 1 can be entered in this entry box. In the next window, overall slope angles are entered. Figure 5.4 shows an example for 4 zones of slope change with respect to azimuth.

Overall slope change with respect to depth

Number of zones

Figure 5.5. Case 3: Entry window for number of zones

	Overall slope angle	Depth (from)	Depth (to)
1.	45	0	50
2.	40	50	100
3.	35	100	150

Figure 5.6. Case 3: Entry window for overall slope angles in different ranges of depth

In case 3, the overall slope angle is not the same in different zones with respect to depth. Spline interpolation is not utilized in this case. If this case is chosen, number of depth zones are entered in the window given in Figure 5.5. Any integer number greater than 1 can be entered in this entry box. In the subsequent window, overall slope angles are entered with the ranges of depth. Unit of depth is in meters. An example of 3 zones of depth is provided in Figure 5.6.

Overall slope change with respect to depth and azimuth

Number of zones for azimuth

Number of zones for depth

Figure 5.7. Case 4: Entry window for number of zones for azimuth and depth

	Overall slope angle	Azimuth (from)	Azimuth (to)
Zone 1	<input type="text"/>	<input type="text"/>	<input type="text"/>
Zone 2	<input type="text"/>	<input type="text"/>	<input type="text"/>
Zone 3	<input type="text"/>	<input type="text"/>	<input type="text"/>
Zone 4	<input type="text"/>	<input type="text"/>	<input type="text"/>
	Overall slope angle	Azimuth (from)	Azimuth (to)
Zone 5	<input type="text"/>	<input type="text"/>	<input type="text"/>
Zone 6	<input type="text"/>	<input type="text"/>	<input type="text"/>
Zone 7	<input type="text"/>	<input type="text"/>	<input type="text"/>
Zone 8	<input type="text"/>	<input type="text"/>	<input type="text"/>
	Overall slope angle	Azimuth (from)	Azimuth (to)
Zone 9	<input type="text"/>	<input type="text"/>	<input type="text"/>
Zone 10	<input type="text"/>	<input type="text"/>	<input type="text"/>
Zone 11	<input type="text"/>	<input type="text"/>	<input type="text"/>
Zone 12	<input type="text"/>	<input type="text"/>	<input type="text"/>

OK

Figure 5.8. Case 4: Entry window for overall slope angles in different azimuth ranges

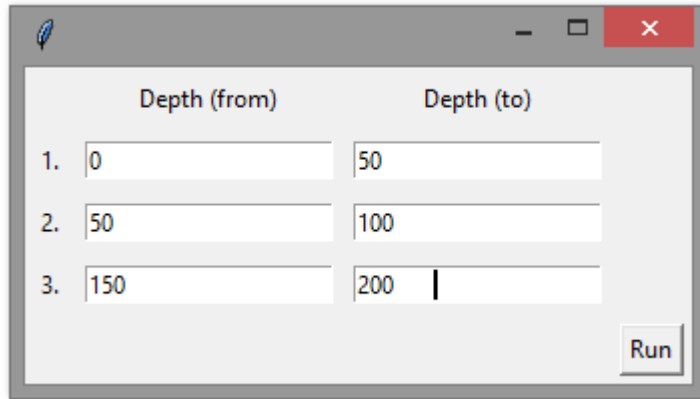


Figure 5.9. Case 4: Entry window for ranges of depth

In case 4, the overall slope angle changes with respect to both depth and azimuth. Spline interpolation is used for this case. The window shown in Figure 5.7 appears if this case is selected. In this window, number of azimuth and depth ranges are entered. After entering the number of zones, the third window pops up. For  $n$  number of azimuth range and  $k$  number of depth range,  $n \times k$  number of overall slope angles must be entered in the third window. An example of  $3 \times 4$  zones is given in Figure 5.8. In the fourth window, ranges of depth are entered (Figure 5.9).

In all cases, after run command is executed, two windows pop up to select a file of block data and a LP file. Block data file must be a MS Excel file which contains block coordinates, block dimensions, and grades. LP file can be created with an empty text file with an extension ".lp". This file defines mathematical model of mixed integer programming written in the code. After selecting these two files, optimization calculations start in the code.

## 5.2. GUI for Output Data

At the end of the optimization process, generated output data are saved in MS Excel files and images, and a LP file is created. Two windows pop up after a solution is found so that two MS Excel files can be saved for extracted and non-extracted blocks. These files contain economic block values, block dimensions, and coordinates of the

blocks. In addition, the code creates two figures which are three dimensional images of extracted blocks and non-extracted blocks. Two examples of these images are demonstrated in Figure 5.10 and 5.11. In these figures, reference point of x, y, and z coordinates are not the same with that of the blocks for the convenience of demonstration. If spline interpolation is required in the calculations, an image of the points created by spline interpolation is also generated (Figure 5.12). In addition, an information message window pops up to show total economic block value and stripping ratio ( $t/m^3$  or  $m^3/m^3$ ) (Figure 5.13). Moreover, mathematical model of mixed integer programming can be read from the LP file, i.e., objective function, decision variables, and constraints can be read from this file.

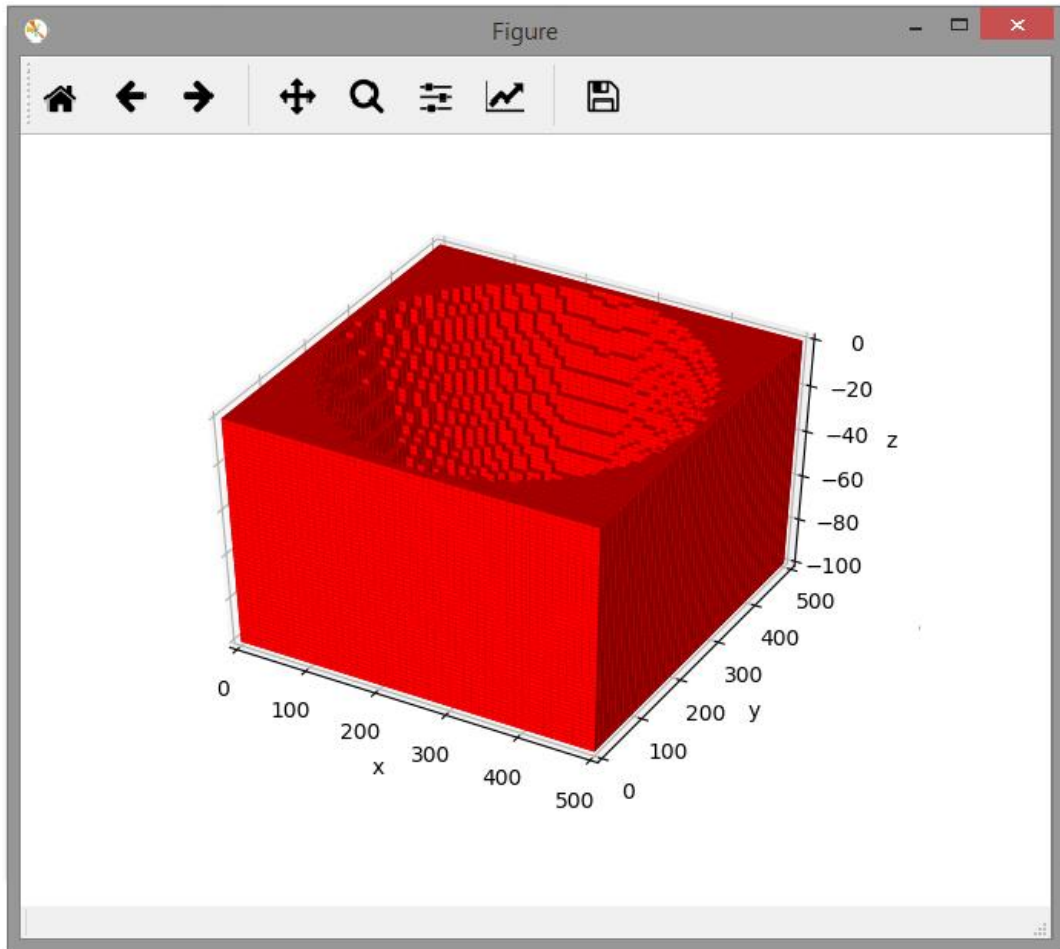


Figure 5.10. Ultimate pit limit of a block model consisting of 125,000 blocks

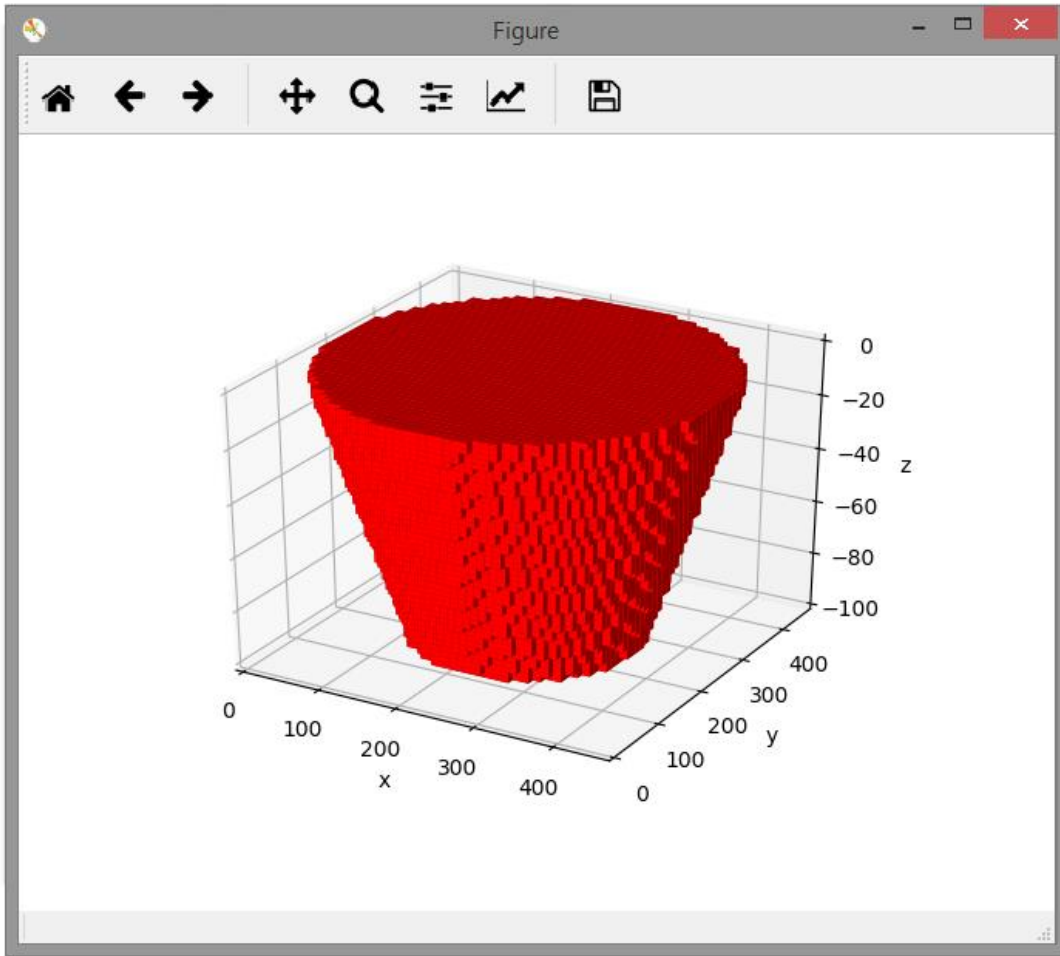


Figure 5.11. Extracted blocks of a block model consisting of 125,000 blocks

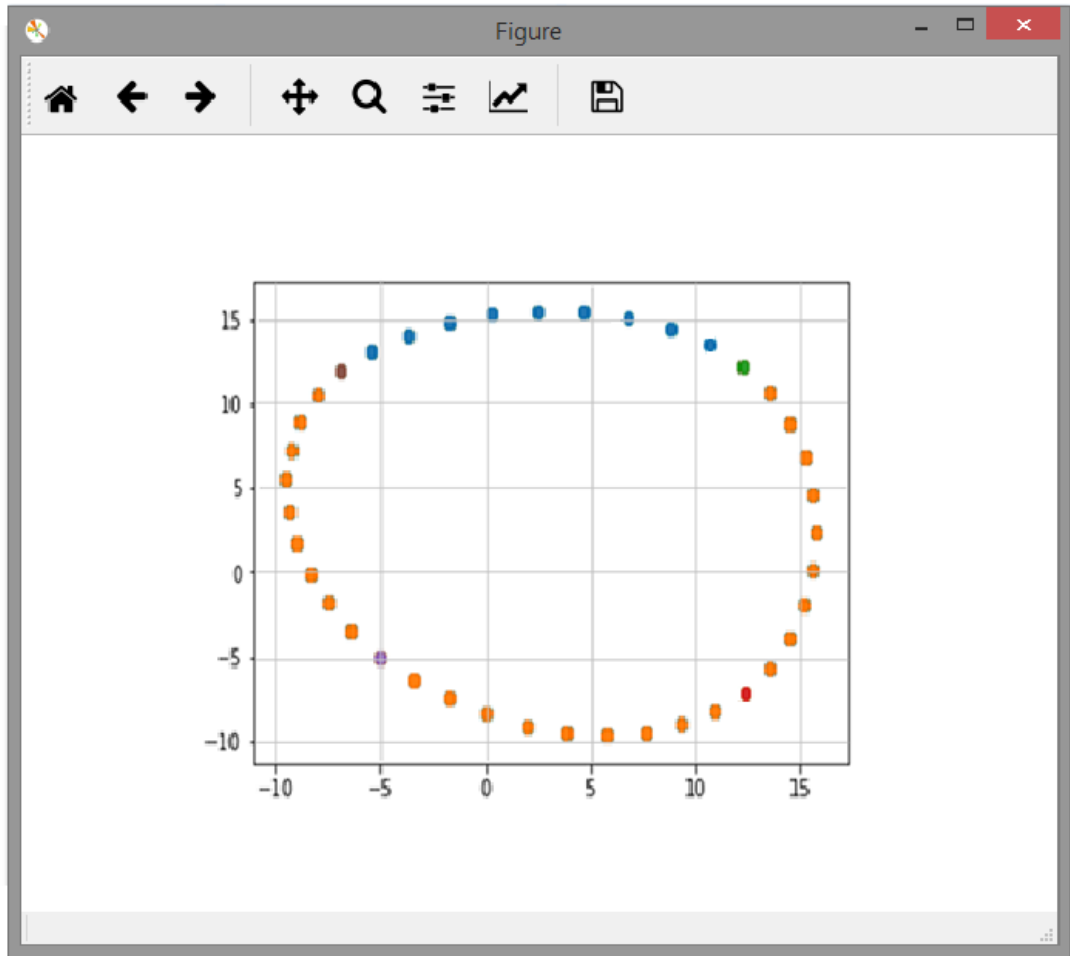


Figure 5.12. The points created by cubic spline interpolation for various overall slope angles

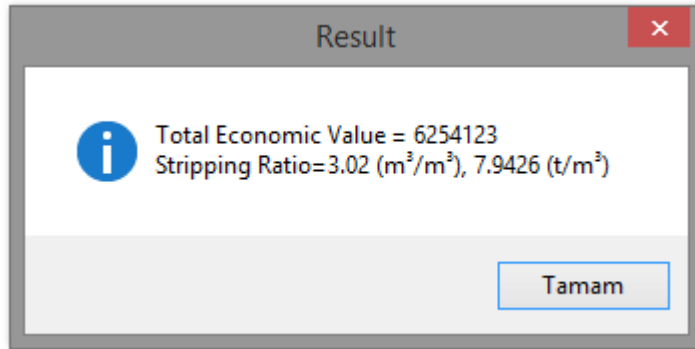


Figure 5.13. Information window for total economic block value and stripping ratio

## CHAPTER 6

### CASE STUDY

In order to validate the applicability of the proposed method, it is applied on the block data obtained from two mine sites. A magnetite orebody, a hematite-magnetite orebody and a lignite orebody are used. For the block models of magnetite and hematite-magnetite orebody, optimization is carried out for the cases in which overall slope angle is constant and overall slope angle changes with respect to azimuth. For the lignite orebody, optimization is performed for the cases in which overall slope angle varies with respect depth and overall slope angle changes with respect to both azimuth and depth. The results are analyzed to check if input and output overall slope angles are the same or similar to each other. The total economic block value (\$), stripping ratio ( $t/m^3$  and  $m^3/m^3$ ) are also provided in the results.

#### 6.1. Magnetite Orebody

##### 6.1.1. Block Model

In this block model, block dimensions are 2.5 m in x, y, and z directions. Waste block dimensions are 2.5, 2.5, and 2.5 m and 10, 10, and 2.5 in the x, y and z directions respectively. The number of blocks is given in Table 6.1. Block model can be seen in Figure 6.1.

Table 6.1. Number of blocks

	<b>Ore blocks</b>	<b>Waste blocks (2.5×2.5×2.5 m<sup>3</sup>)</b>	<b>Waste blocks (10×10×2.5 m<sup>3</sup>)</b>	<b>Total</b>
<b>Number of blocks</b>	59,391	20,210	8,325	87,926

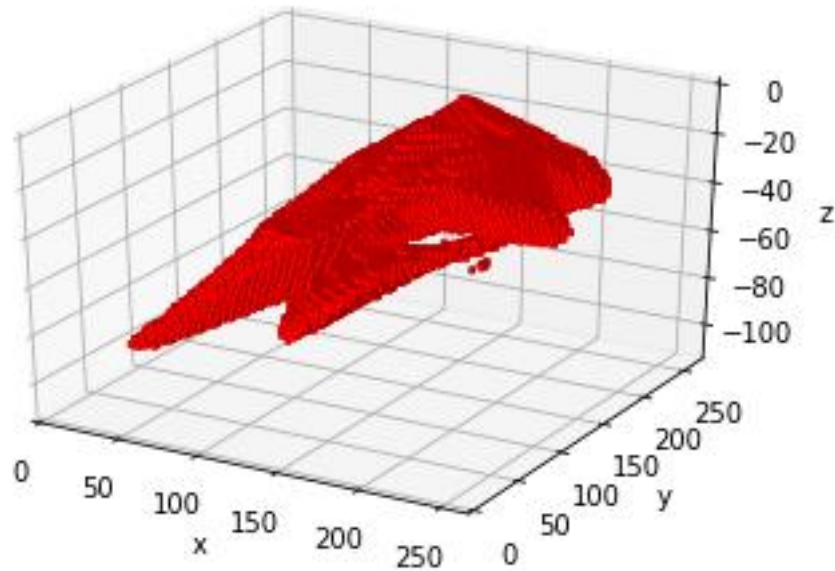


Figure 6.1. Block model of the magnetite orebody

### 6.1.2. Economic Block Value and Input Data

To calculate economic block value, price, selling cost, mining cost, and processing cost are assumed as 85, 5, 5, and 5 \$/tonne respectively (Figure 6.2). Average density is  $3.73 \text{ g/cm}^3$  for ore blocks. Average density for waste blocks is assumed as  $2.63 \text{ g/cm}^3$  in all cases. Bench height is 10 m and bench face angle is  $80^\circ$ . For this case, overall slope angle is constant, and it is equal to  $30^\circ$ .

Economic Block Value Parameters		Choose One of the Cases:	
Price	85	<input checked="" type="checkbox"/>	Constant overall slope angle
Selling cost	5	<input type="checkbox"/>	Overall slope change with respect to azimuth
Mining cost	5	<input type="checkbox"/>	Overall slope change with respect to depth
Processing cost	5	<input type="checkbox"/>	Overall slope change with respect to depth and azimuth
Average density	3.73	<b>3D Figures</b>	
Mining cost increase per meter of depth	0.03	<input checked="" type="radio"/>	Display the final pit
Recovery	90	<input type="radio"/>	Display the extracted blocks
<b>Bench Parameters</b>			
Bench height	10		
Bench face angle	80		

Figure 6.2. Economic block value parameters for case 1

### 6.1.3. Results

After completion of optimization process, it was found that stripping ratio is 3.92 m<sup>3</sup>/m<sup>3</sup> (10.310 t/m<sup>3</sup>) and total economic block value is 61,038,764 \$ (Table 6.2). Extracted blocks are demonstrated in Figure 6.3. In Figure 6.4, N-S section of the extracted blocks can be seen. The measured overall slope angles are 30.548° and 30.964° which are close to the angle entered (30°). The figures of the other sections and comparison between entered and measured overall slope angles are given in Appendix C. The difference between measured and the angle entered are between 0.051° and 0.964°.

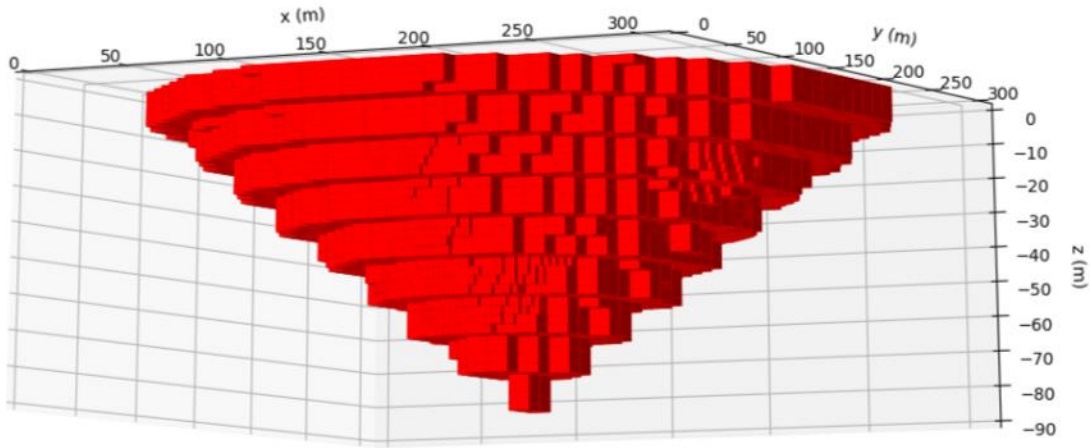


Figure 6.3. Extracted blocks

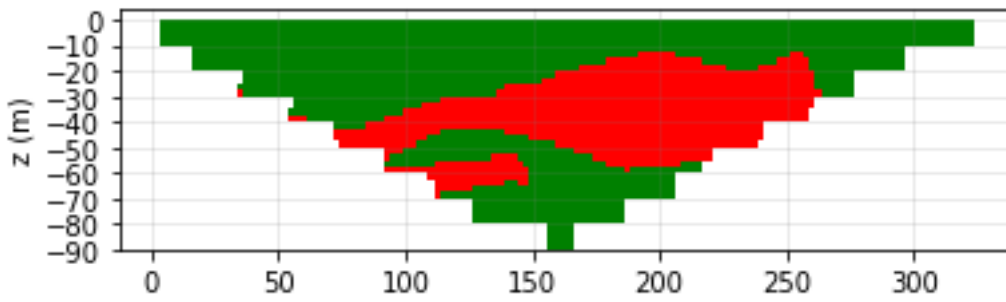


Figure 6.4. N-S section of the extracted blocks

Table 6.2. Output data

<b>Stripping ratio</b>	3.920 m <sup>3</sup> /m <sup>3</sup> , 10.310 t/m <sup>3</sup>
<b>Total economic block value</b>	61,038,764 \$

## 6.2. Magnetite-hematite Orebody

### 6.2.1. Block Model

In this block model, block dimensions are 2.5 m in x, y, and z directions. Waste block dimensions are 2.5, 2.5, and 2.5 m and 10, 10, and 2.5 m in the x, y and z directions, respectively. Bench height is 10 m and bench face angle is  $80^{\circ}$ . The number of blocks is given in Table 6.3. Block model can be seen in Figure 6.5.

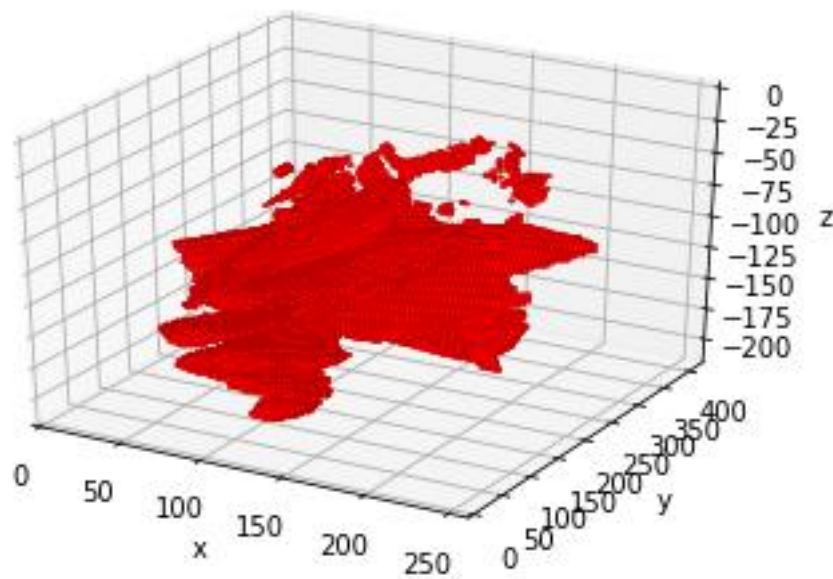


Figure 6.5. Block model of the magnetite-hematite orebody

Table 6.3. Number of blocks

	<b>Ore blocks</b>	<b>Waste blocks (<math>2.5 \times 2.5 \times 2.5 \text{ m}^3</math>)</b>	<b>Waste blocks (<math>10 \times 10 \times 2.5 \text{ m}^3</math>)</b>	<b>Total</b>
<b>Number of blocks</b>	40,600	27,033	104,190	171,823

### 6.2.2. Economic Block Values and Input Data

For the magnetite orebody, to compute economic block value, price, selling cost, mining cost, and processing cost, are assumed as 85, 5, 5, and 5 \$/tonne, respectively (Figure 6.6). Bench height is 10 m and bench face angle is  $80^{\circ}$ . Average density is entered as  $4.19 \text{ g/cm}^3$ . For this case, overall slope angle changes with respect to azimuth. The input values for overall slope angles are given in Table 6.4. Since overall slope angle changes with respect to azimuth, spline interpolation is used in this case. The curve formed by spline interpolation is shown in Figure 6.7.

Economic Block Value Parameters		Choose One of the Cases:	
Price	85	<input type="checkbox"/>	Constant overall slope angle
Selling cost	5	<input checked="" type="checkbox"/>	Overall slope change with respect to azimuth
Mining cost	5	<input type="checkbox"/>	Overall slope change with respect to depth
Processing cost	5	<input type="checkbox"/>	Overall slope change with respect to depth and azimuth
Average density	4.19	3D Figures	
Mining cost increase per meter of depth	0.03	<input type="checkbox"/>	Display the final pit
Recovery	90	<input type="checkbox"/>	Display the extracted blocks
Bench Parameters			
Bench height	10		
Bench face angle	80		

Figure 6.6. Economic block value and bench parameters for case 2

Table 6.4. Overall slope angles

Overall slope angle	Azimuth (from)	Azimuth (to)
55	346	79
41	79	166
58	166	259
51	259	346

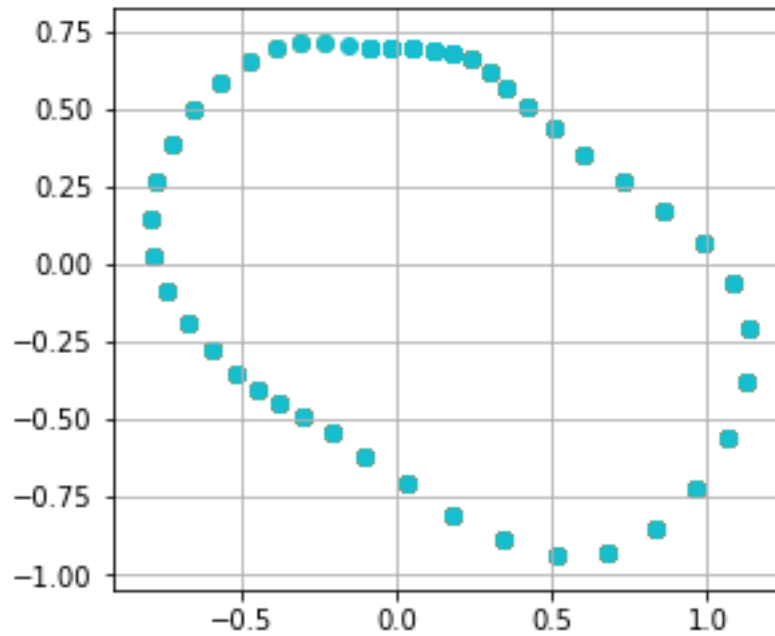


Figure 6.7. The curve formed by spline interpolation for case 2

### 6.2.3. Results

According to the result of optimization, stripping ratio is  $17.530 \text{ m}^3/\text{m}^3$  ( $46.104 \text{ t/m}^3$ ) and total economic block value is  $22,706,767$  \$. Extracted blocks are shown in Figure 6.8. N 45 E section of the extracted blocks is demonstrated in Figure 6.9. The figure of the other cross section and comparison of overall slope angles are given in

Appendix C. The difference between entered and measured overall slope angles changes is between  $0.058^\circ$  and  $1.479^\circ$ .

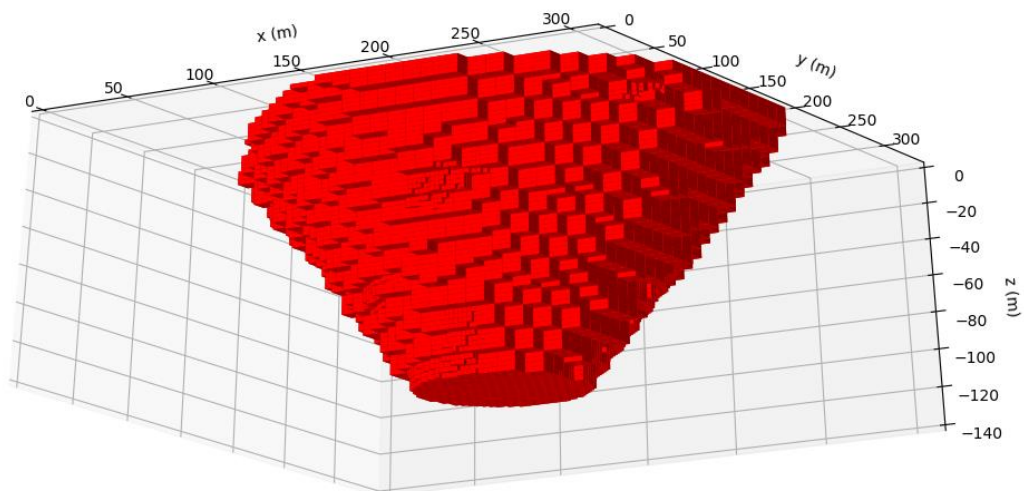


Figure 6.8. Extracted blocks

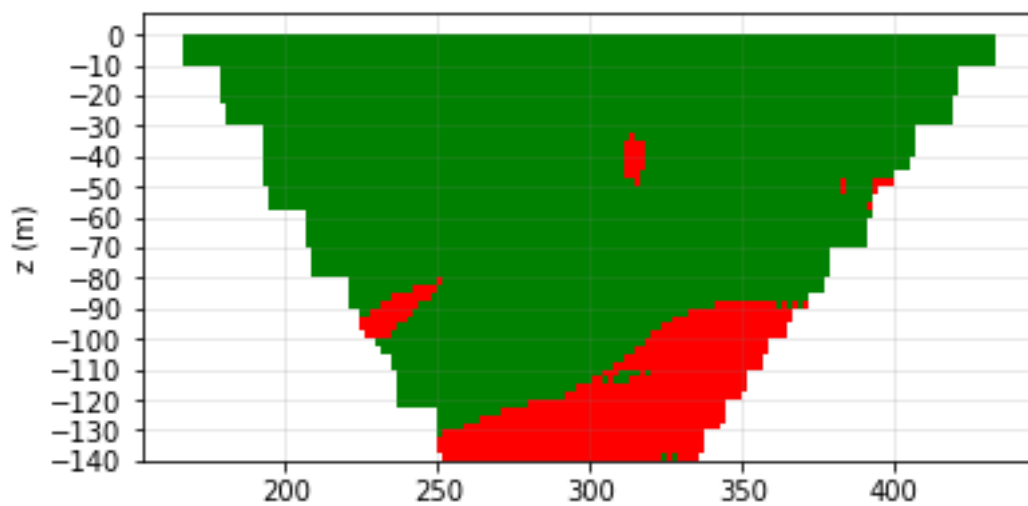


Figure 6.9. N 45 E section of the extracted blocks

Table 6.5. Output data

<b>Stripping ratio</b>	17.530 m <sup>3</sup> /m <sup>3</sup> , 46.104 t/m <sup>3</sup>
<b>Total economic block value</b>	22,706,767 \$

### 6.3. Lignite Orebody 1

#### 6.3.1. Block Model

In this block model, block dimensions are 10, 10, and 2 m in x, y, and z directions, respectively. Waste block dimensions are 10, 10, and 2 m and 20, 20, and 2 in the x, y and z directions, respectively. The number of blocks is given in Table 6.6. The block model can be seen in Figure 6.10.

Table 6.6. Number of blocks

	<b>Ore blocks</b>	<b>Waste blocks (10×10×2 m<sup>3</sup>)</b>	<b>Waste blocks (20×20×2 m<sup>3</sup>)</b>	<b>Total</b>
<b>Number of blocks</b>	66,350	3,503	26,118	95,971

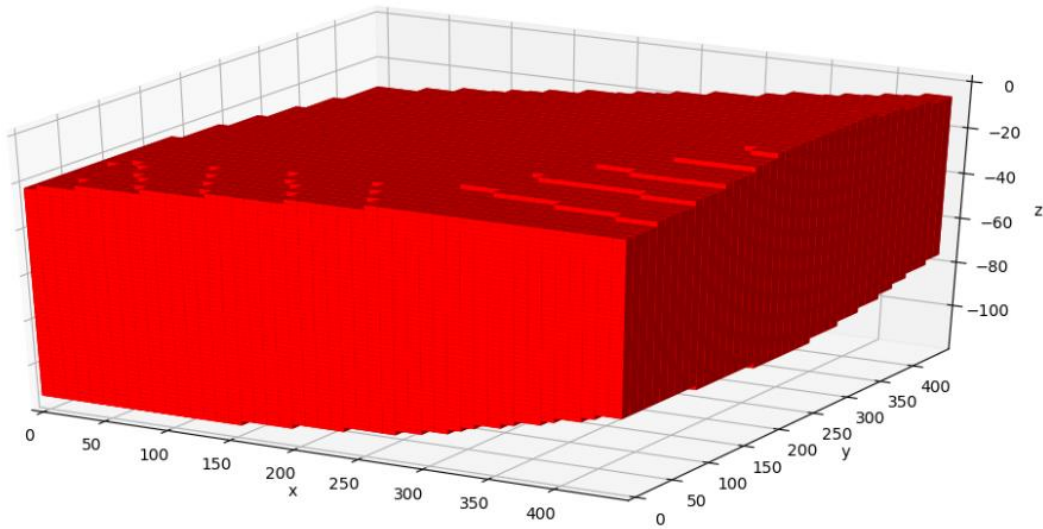


Figure 6.10. Block model of the lignite orebody

### 6.3.2. Economic Block Values and Input Data

To determine economic block value, price, selling cost, mining cost, processing cost are assumed as 30, 1, 1, and 1 \$/tonne, respectively (Figure 6.11). Average density is  $2.19 \text{ g/cm}^3$ . Bench height is 10 m and bench face angle is  $60^\circ$ . For this case, overall slope angle changes with respect to depth and the depth ranges are given in Table 6.7.

**Economic Block Value Parameters**

Price: 30

Selling cost: 1

Mining cost: 1

Processing cost: 1

Average density: 2.19

Mining cost increase per meter of depth: 0.03

Recovery: 90

**Bench Parameters**

Bench height: 10

Bench face angle: 60

**Choose One of the Cases:**

Constant overall slope angle

Overall slope change with respect to azimuth

Overall slope change with respect to depth

Overall slope change with respect to depth and azimuth

**3D Figures**

Display the final pit

Display the extracted blocks

OK

Figure 6.11. Economic block value and bench parameters for case 3

Table 6.7. Input data for depth ranges

Overall slope angle	Depth (from)	Depth (to)
25	0	40
20	40	80

### 6.3.3. Results

From the results of the optimization, stripping ratio is found as  $10.073 \text{ m}^3/\text{m}^3$  ( $26.492 \text{ t}/\text{m}^3$ ) and total economic block value is 35,734,525 \$. Extracted blocks are shown in Figure 6.12. In Figure 6.13, N-S section of the extracted blocks can be seen. The figures of the other section and overall slope angles in the other sections are given in Appendix C. The difference between measured and entered overall slope angles is between  $0.051^\circ$  and  $0.964^\circ$ .

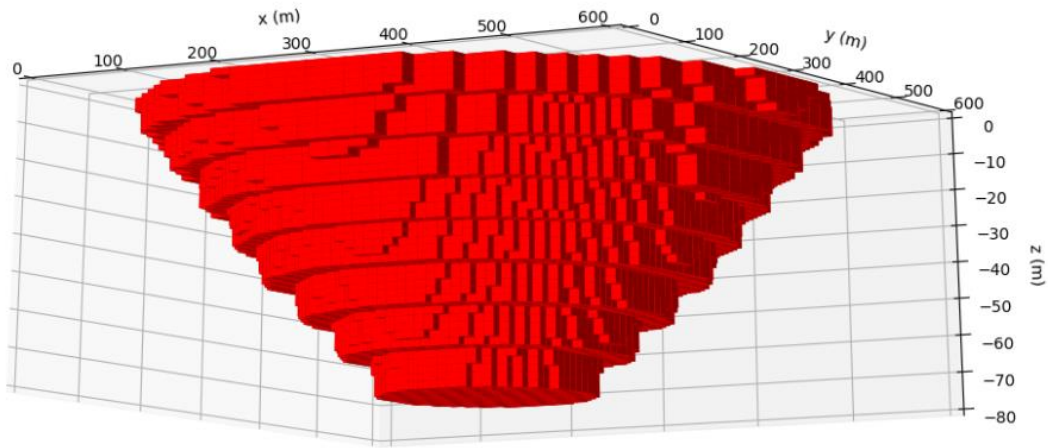


Figure 6.12. Extracted blocks

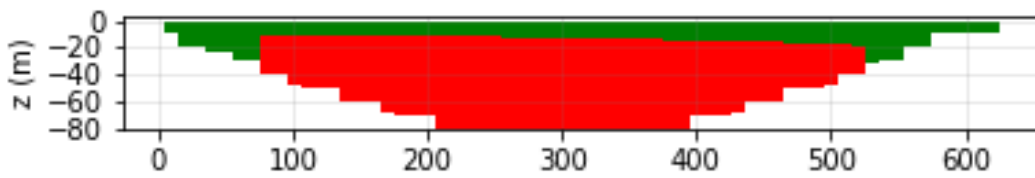


Figure 6.13. N-S section of the extracted blocks

Table 6.8. Output data

<b>Stripping ratio</b>	10.073 m <sup>3</sup> /m <sup>3</sup> , 26.492 t/m <sup>3</sup>
<b>Total economic block value</b>	35,734,525 \$

## 6.4. Lignite Orebody 2

### 6.4.1. Economic Block Values and Input Data

In this case, economic block value parameters, bench parameters, and the block model are the same as those given in the part 6.3, but the overall slope angle changes with respect to both depth and azimuth. Overall slope angles, azimuths and depth ranges are given in Table 6.9. In this case, spline interpolation is also used, and the curve created by spline interpolation can be seen in Figure 6.14.

Table 6.9. Input data for depth range, overall slope angle, and azimuth

<b>Depth Range (m)</b>	<b>Overall slope angle</b>	<b>Azimuth (from)</b>	<b>Azimuth (to)</b>
0-40	35	0	90
	30	90	180
	38	180	270
	31	270	360
40-80	25	0	90
	20	90	180
	28	180	270
	21	270	360

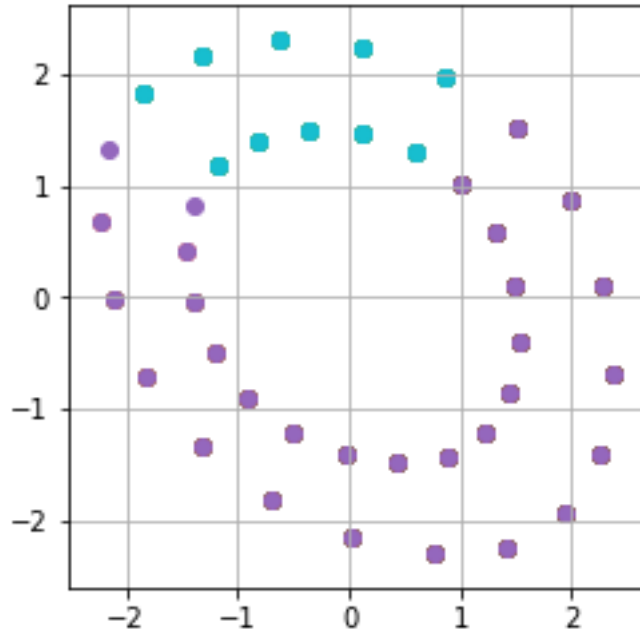


Figure 6.14. The curve formed by spline interpolation for case 4

#### 6.4.2. Results

It was found that stripping ratio is  $15.256 \text{ m}^3/\text{m}^3$  ( $40.833 \text{ t}/\text{m}^3$ ) and total economic block value is 16,884,309 \$. Extracted blocks are shown in Figure 6.15. In Figure 6.16, N 45 E section of the extracted blocks is presented. The other cross section and overall slope angles are given Appendix C. The difference between measured and entered overall slope angles are between  $0.265^\circ$  and  $5.264^\circ$ . The difference is large because depth is smaller than 100 m and number of the blocks is smaller in this case, which makes it hard to obtain the angle entered.

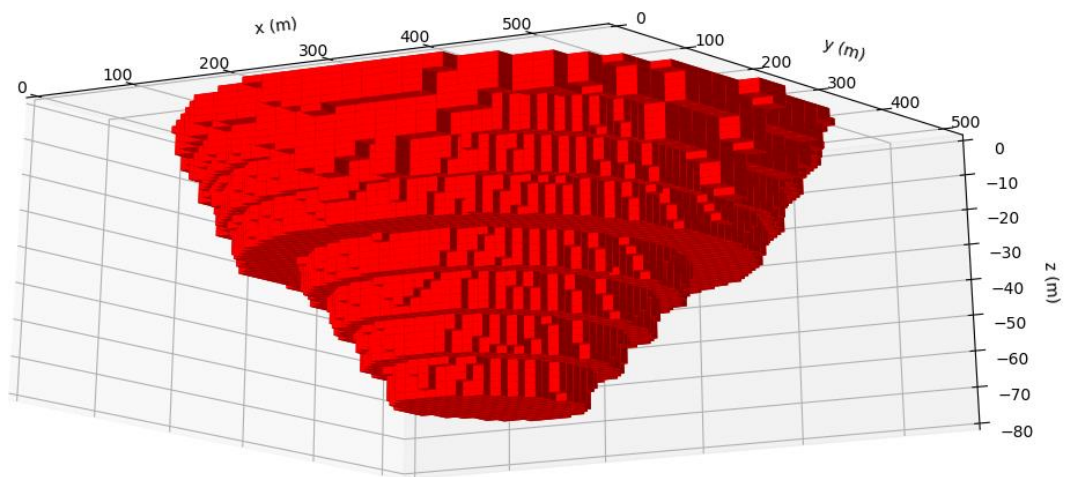


Figure 6.15. Extracted blocks

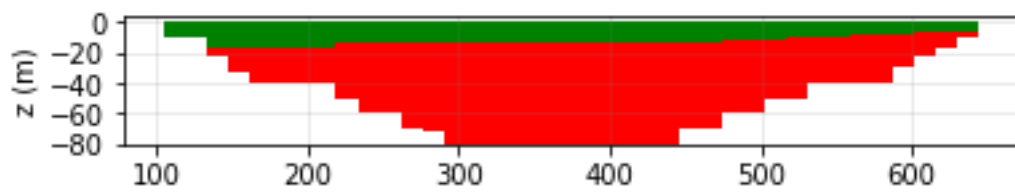


Figure 6.16. N 45 E section of the extracted blocks

Table 6.10. Output data

<b>Stripping ratio</b>	15.526 m <sup>3</sup> /m <sup>3</sup> , 40.833 t/m <sup>3</sup>
<b>Total economic block value</b>	16,884,309 \$



## CHAPTER 7

### CONCLUSION AND RECOMMENDATIONS

Ultimate pit limit is determined in order to find out the final outline of the open pit mine with undiscounted value of money. The final pit limit which gives maximum economic value while considering technical and safety issues is found. For this purpose, many optimization techniques of ultimate pit limit were developed. In these proposed methods, generally, constant overall slope angles are used in the optimization. Thus, a new approach was proposed to overcome this problem. In the proposed method, mixed integer programming was used for optimization. The spline interpolation was used to obtain different overall slope angles in the mathematical model. In addition, bench height and bench face angle were incorporated in the optimization. The method was coded in Python Programming language and graphical user interface was also formed for easier application.

Firstly, the code was applied by using hypothetical block models consisting of 86100, 107916, 118096, 494900 blocks to verify the mathematical model. Input data for overall slope angles are compared to overall slope angles obtained from output data. It was found that the angles are the same or close to each other. The difference between input and measured values are between  $0^{\circ}$  to  $8^{\circ}$  and the difference is mostly between  $0^{\circ}$  and  $2^{\circ}$ . However, the difference between required angles and generated angles by the code becomes smaller as the number of the blocks increases. When generating a curvilinear pit shape with flat edges of a block, the difference between input and output angles is expected to be large if the number of blocks is too small. The gap between the input and output angles are between 0 and 1 if number of blocks is much greater than 100,000. However, required angle can be obtained even if number of blocks is lower than 100,000. This is because the generated angle also depends on bench height, bench width and block dimensions.

For the example with 494,900 blocks, parameters which give high economic block values are entered in the GUI so that the run time is shorter. This enabled the code to reach a solution for this block model.

After the mathematical model is verified, the method was applied on the data obtained from magnetite, hematite and lignite ore deposits. It is observed that the run time is higher when the model is applied for the real mine site because number of waste blocks are high. To deal with this problem, dimensions of some of the waste blocks are increased to lower the number of blocks so that computation time can be decreased.

According to the results of the case studies, difference between input and output value of overall slope angles changes from 0.017 to 5.264. It is observed that this difference is higher in shallow depth ranges. This is because there are larger-sized waste blocks on upper levels.

It can be concluded from the results that the proposed technique can be a useful option for incorporation of various overall slope angles into the optimization of ultimate pit limit. Advantage of this proposed technique is that pit shape with desired overall slope angles and maximum economic value are simultaneously obtained. The pit with the required overall slope angle is not formed after the optimization calculations finish. However, it has some aspects that must be improved. They can be presented as follows:

- The proposed method requires high computational time. To deal with this problem, other methods can be utilized instead of mixed integer programming.
- In the model, topography is not taken into consideration. For more realistic design, topographical data should be included in the model.
- The case in which overall slope angle decreases as the pit deepens is not included in the code. However, various overall slope angles can be given in different depth ranges in the code.
- Bench width is included in the model, but haulage roads can also be added in the geometrical equations.

- In this method, time value of money is not considered for ultimate pit limit problem. However, if the problem in computation time is resolved, it can be an alternative method in long-term production planning.
- Economic calculations can be done in a more detailed way.
- Other aspects related to rock mechanics can be included in the code.



## REFERENCES

- Abbaspour, H. (2011). Optimum Ultimate Pit Limit (UPL) Design by Graph Theory (Doctoral dissertation, Tese (Douto)).
- Achireko, PK. (1998). Application of modified conditional simulation and artificial neural networks to open pit optimization. Ph.D. Dissertation, Technical University of Nova Scotia, Canada.
- Akaike, A. and Dagdelen, K. (1999). A strategic production scheduling method for an open pit mine. Paper presented at the Proceedings of the 28th International Symposium on Application of Computers & Operations Research in the Mineral Industry.
- Albor Consuegra, F. R. and Dimitrakopoulos, R. (2010). Algorithmic approach to pushback design based on stochastic programming: Method, application and comparisons. *Mining Technology*. 119. 88-101.
- Asa, E. (2002). An intelligent 3-d open pit design and optimization using machine learning - adaptive logic networks and neuro-genetic algorithms, 43-45.
- Auger G. (2000). Programming the maximum flow algorithm applied to the ultimate contour problems in open pit mines. MSc. Dissertation, École Polytechnique de Montréal
- Barnes, R. J., and Johnson, T. B. (1982). Bounding techniques for the ultimate pit limit problem. In *Application of Computers and Operations Research in the Mineral Industry*. Soc of Min Eng of AIME, 263-273
- Caccetta, L. and Giannini, L. (1988). An application of discrete mathematics in the design of an open pit mine. *Discrete Applied Mathematics*, 21(1), 1-19.
- Caccetta, L. and Hill, S. P. (2003). An application of branch and cut to open pit mine scheduling. *Journal of global optimization*, 27(2-3), 349-365.
- Caccetta, L., Kelsey, P. and Giannini, L. (1998). Open pit mine production scheduling. Paper presented at the APCOM 98: Computer Applications in the Mineral Industries International Symposium.

- Carlson, T. R., Erickson, J. D., O'Brain D. T. and Pana, M. T. (1966). Computer techniques in mine planning, *Mining Engineering*, Vol. 18, No. 5, 53-56.
- Chen, T. (1977). 3D pit design with variable wall slope capabilities. Proc. 141\*1 APCOM. AIME. New-York, 615-625.
- Coléou, T. (1988). Technical parameterization for open pit design and mine planning. Paper presented at the Proc. 21st APCOM Symposium of the Society of Mining Engineers (AIME). 485-494
- Dagdelen, K. and Johnson, T. B. (1986). Optimum open pit mine production scheduling by lagrangian parameterization. Paper presented at the 19th APCOM Symposium of the society of mining engineers (AIME).
- Denby, B., and Schofield, D. (1994). Open pit design and scheduling by use of genetic algorithms. *Transactions of the Institution of Mining and Metallurgy. Section A. Mining Industry*, 103.
- Dowd, P. and Onur, A. (1992). Optimising open pit design and sequencing. Paper presented at the Proc. 23rd International APCOM Symposium.
- Dowd, P. and Onur, A. (1993). Open-pit optimization- part 2: Production scheduling and inclusion of roadways. *TRANS INST MIN METAL SECT A MIN IND.*, 102, 105-113.
- Elahizeyni, E., Kakaie, R. and Yousefi, A. (2011). A new algorithm for optimum open pit design: Floating cone method III, *Journal of Mining & Environment*, Vol.2, No.2, 118-125.
- Erarslan, K. (1996). Development of a model for open pit limits optimization integrated with a sequencing system, PhD Thesis, METU
- Erarslan, K., and Celebi, N. (2001). A simulative model for optimum open pit design. *CIM BULLETIN*, 94(1055), 59-68.
- Francois-Bongarcon, D. and Guibal, D. (1982). Algorithms for parameterizing reserves under different geometrical constraints. Paper presented at the Proc.

17th symposium on the application of computers and operations research in the mineral industries (APCOM: AIME).

Francois-Bongarcon, D. and Guibal, D. (1984). Parameterization of optimal designs of an open pit-beginning of a new phase of research. Transactions of the Society of Mining Engineers of AIME, 274, 1801-1805.

Francois-Bongarcon, D. and Marechal, A. (1976). A new method for open pit design: Parametrization of the final pit contour. Paper presented at the APCOM symposium.

Frimpong, S. Whiting J. M., and Szymanski, J. (1998). Stochastic-optimization annealing of an intelligent open pit design, Miner. Resour. Eng., vol. 7, no. 1, 15-27.

Gershon, M. (1987). Heuristic approaches for mine planning and production scheduling. International Journal of Mining and Geological Engineering, 5(1), 1-13.

Gershon, M. E. (1983). Optimal mine production scheduling: Evaluation of large scale mathematical programming approaches. International Journal of Mining Engineering, 1(4), 315-329.

Giannini, L. (1990). Optimum design of open pit mines. PhD Dissertation, Curtin University of Technology, Perth.

Graphical User Interfaces with Tk. (n. d.). Retrieved from <https://docs.python.org/3/library/tk.html>

Haupt, R.L. and Haupt, S.E. (2004). Practical Genetic Algorithms., John Wiley and Sons: USA.

Held, M., Wolfe, P. and Crowder, H. P. (1974). Validation of subgradient optimization. Mathematical Programming, 6(1), 62-88.

Hochbaum, D. S., and Chen, A. (2000). Performance analysis and best implementations of old and new algorithms for the open pit mining problem. Operation research, 48(6), 894-914.

- Hustrulid, W. and Kuchta, M. (2016). Open pit mine planning and design. Volume 1 – fundamentals. Netherlands.
- Huttagosol, P. (1988). Modified tree graph algorithm for ultimate pit limit analysis. MSc Dissertation, Colorado School of Mines, Golden Colorado.
- Johnson, T. B. (1968). Optimum open pit mine production scheduling. California University, Berkeley, Operations Research Center.
- Johnson, T. B. (1969). Optimum production scheduling. Proceedings of the 8th International Symposium on Computers and Operations Research. 539-562.
- Johnson, T. B. and Sharp, W. R. (1971). A three-dimensional dynamic programming method for optimal ultimate open pit design (Vol. 7553): Bureau of Mines, US Dep. of the Interior.
- Khalokakaie, R. (1999). Computer-Aided Optimal Open Pit Design with Variable Slope Angles, PhD Thesis, University of Leeds.
- Khalokakaie, R. (2006). Optimum open pit design with modified moving cone II methods, Journal of engineering in Tehran university, Vol. 4, No. 3 ,297-307.
- Khan, A. and Niemann-Delius, C. (2014). Production scheduling of open pit mines using particle swarm optimization algorithm. Advances in Operations Research, 2014.
- Koenigsberg, E. (1982). The optimum contours of an open pit mine: an application of dynamic programming. 17th APCOM Symposium, Society of Mining Engineers of AIME: New York (USA), 274-287.
- Kumral, M., and Dowd, P. A. (2004). A simulated annealing approach to mine production scheduling. Journal of the Operational Research Society, 56(8), 922-930.
- Lerchs, H. and Grossman, I.F. (1965). Optimum design of open pit mines. Can. Inst. Min. Bull., vol. 58, 47-54.

- Lipkewich, M. P. and Borgman, L. (1969). Two- and three-dimensional pit design optimization techniques. A Decade of Digital Computing in the Mineral Industry. AIME, New York, 505-523.
- Liu, S. Q. and Kozan E. (2016). New graph-based algorithms to efficiently solve large scale open pit mining optimization problems. Expert Systems with Applications. 59-65. Volume 43.
- Math-Mathematical functions. (n. d.). Retrieved from <https://docs.python.org/3/library/math.html>
- Matheron, G. (1975). Le paramétrage des contours optimaux. Technique notes, 401, 19-54.
- Matplotlib. (n. d.). Retrieved from <https://matplotlib.org/>
- Milani, G. (2016). A Genetic Algorithm with Zooming for the Determination of the Optimal Open Pit Mines Layout. The Open Civil Engineering Journal. 10. 301-322.
- Nogholi, A. (2015). Optimisation of open pit mine block sequencing. PhD Dissertation. Queensland University of Technology.
- NumPy. (n. d.). Retrieved from <https://numpy.org/>
- Osanloo, M., Gholamnejad, J. and Karimi, B. (2008). Long-term open pit mine production planning: A review of models and algorithms. International Journal of Mining, Reclamation and Environment, 22(1), 3-35.
- Özkan, M. (2015). A new algorithm for open pit mine production planning. PhD Thesis. ITU.
- Pana, M.T. (1965). The simulation approach to open-pit design. Proc. s"1 APCOM. 2. Tucson, Arizona, ZZ1-24.
- Picard, J.C. (1976). Maximum closure of a graph and applications to combinatorial problems. Management Science. 22. No 11,1268-1272.
- PuLP 1.6.10. (n. d.). Retrieved from <https://pypi.org/project/PuLP/>

Python Data Analysis Library. (n. d.). Retrieved from <https://pandas.pydata.org/>

Ramazan, S., Dagdelen, K. and Johnson, T. (2005). Fundamental tree algorithm in optimising production scheduling for open pit mine design. *Mining Technology*, 114(1), 45-54.

Roman, R. (1974). The role of time value of money in determining an open pit mining sequence and pit limits. Paper presented at the 12th Apoom Symposium.

Rychkun, E., and Chen, T. (1979). Open Pit Mine Feasibility Method and Application at Placer Development. *Computer Methods for the 80's in the Mineral Industry*, 80, 304-309.

Salomon D. (2006). *Curves and surfaces for computer graphics*. Springer-Verlag New York Inc.

Sandi, C. (1979). Subgradient optimization. *Combinatorial optimization*. 73-91.

Sattarvand, J. and Shisvan, M. S. (2012). Modelling of Accurate Variable Slope Angles in Open-Pit Mine Design Using Spline Interpolation. *Archives of Mining Sciences*. 57(4). 921-932.

Sayadi, Ahmad Reza and Fathianpour, Nader & Mousavi, Amin. (2011). Open pit optimization in 3D using a new artificial neural network. *Archives of Mining Sciences*. 56. 389-403.

Sevim, H. and Lei, D. D. (1994). The state of long term production planning in open pit mining. Paper presented at the Proceedings of the 3rd International Symposium on Mine Planning and Equipment Selection, October, Istanbul.

Shenggui, Z. and Starfield, A.M. (1985). Dynamic programming with colour graphics smoothing for open pit design on a personal computer. *Geotech. Geol. Eng.*, vol. 3, no. 1, 27-34.

Stuart, N.J. (1992). Pit optimisation using solid modelling and the Lerchs Grossman algorithm. *International Journal of Surface Mining and Reclamation*, & No 1, 19-29.

- Tachefine, B.O., Soumis, F. and Vanderstraten, G. (1993). Decomposition flow algorithm for the operations planning problem in open pit mines. Proc. 24<sup>th</sup> APCOM. 140-147.
- Thomas, G. (1996). Pit optimization and mine production scheduling-the way ahead. Paper presented at the Proc. 26th APCOM Symposium of the Society of Mining Engineers.
- Underwood, R., and Tolwinski, B. (1998). A mathematical programming viewpoint for solving the ultimate pit problem. European Journal of Operational Research, 107(1), 96-107.
- Wang, Q. and Sevim, H. (1992). Enhanced production planning in open pit mining through intelligent dynamic search. Institute of Mining Metallurgy (ed), 23, 461-471.
- Whittle, J. (1993). Four-d whittle open pit optimisation software-user manual. Melbourne, Whittle Programming Pty Ltd.
- Whittle, J. (1998). Four-x user manual. Melbourne: Whittle Programming Pty Ltd.
- Wilke, F.L. and Wright,E.A. (1984). Determining the optimal ultimate pit design for hard rock open pit mines using dynamic programming, Erzmetall, vol. 37, 139-144.
- Wright, E. A. (1999). Moving cone II - A Simple Algorithm for Optimum Pit Limits Design, Proceedings of the 28th Symposium on the application of computers and Operations research in the mineral industries (APCOM), (Colorado USA), 367-374.
- Wyllie, D. C. and Mah, C. W. (2004). Rock slope engineering civil and mining.4th Ed. Spon Press: New York.
- Zhao, Y. and Kim, Y.C. (1992). A new optimum pit limit design algorithm. Proc. 23 APCOM, 423-434.



## APPENDICES

### A. PSEUDOCODE FOR SPLINE INTERPOLATION

Convert angles to x and y points:

for each overall slope angle entered:

convert overall slope angle to radius:

$$r = \frac{1}{\tan \beta}$$

for each radius calculated :

do the following calculations:

$$x^2 = r^2 - y^2$$

$$y = x \cot \alpha$$

$$x = \pm \frac{h}{\tan \beta \sqrt{1 + \cot^2 \alpha}}$$

Form a list of x and y points

Find the inverse of the following matrix:

$$\begin{bmatrix} 1 & 4 & 1 & \dots & 0 & \dots & 0 \\ 0 & 1 & 4 & 1 & \dots & \dots & 0 \\ & & & \ddots & \ddots & & \vdots \\ 0 & \dots & \dots & \dots & 1 & 4 & 1 \\ 1 & \dots & \dots & \dots & 0 & 1 & 4 \\ 4 & 1 & 0 & \dots & 0 & 0 & 1 \end{bmatrix}_{(n \times n)}$$

For each x and y points:

Create the following matrix and substitute x and y points separately:

$$\begin{bmatrix} 3 (P_3 - P_1) \\ 3 (P_4 - P_2) \\ \vdots \\ 3 (P_{n+1} - P_{n-1}) \\ 3 (P_{n+2} - P_n) \end{bmatrix}$$

Do the following calculation to determine  $P_k^t$  values:

$$\begin{bmatrix} 1 & 4 & 1 & \dots & 0 & \dots & 0 \\ 0 & 1 & 4 & 1 & \dots & \dots & 0 \\ & & & \ddots & \ddots & & \vdots \\ 0 & \dots & \dots & \dots & 1 & 4 & 1 \\ 1 & \dots & \dots & \dots & 0 & 1 & 4 \\ 4 & 1 & 0 & \dots & 0 & 0 & 1 \end{bmatrix}^{-1} \cdot \begin{bmatrix} 3 (P_3 - P_1) \\ 3 (P_4 - P_2) \\ \vdots \\ 3 (P_{n+1} - P_{n-1}) \\ 3 (P_{n+2} - P_n) \end{bmatrix}$$

Form the polynomial functions using  $P_k^t$  values

Create a list of parameter whose values are between 0 and 1:

$$t=[0, 0.2, 0.4, 0.6, 0.8]$$

Insert the values of the parameter list in the polynomial functions

Convert x and y points found by interpolation to azimuths and overall slope angles:

for each x and y points found by interpolation:

Do the following calculations:

$$M=\sqrt{x^2 + y^2}$$

$$\text{overall slope angle}=\tan^{-1}(1/M)$$

if  $x>0$  and  $y>0$ :

$$\text{azimuth}=\tan^{-1}(y/x)$$

if  $x<0$  and ( $y>0$  or  $y<0$ ):

$$\text{azimuth} =180+\tan^{-1}(y/x)$$

if  $x>0$  and  $y<0$ :

$$\text{azimuth} =360+\tan^{-1}(y/x)$$

## B. RESULTS OF THE ITERATIONS FOR THE CASE STUDIES

Table B.1. Case study 1

<b>Number of Benches</b>	<b>Total Economic Block Values (\$)</b>
<b>1</b>	135,242
<b>2</b>	7,875,328
<b>3</b>	25,823,166
<b>4</b>	34,915,817
<b>5</b>	47,498,506
<b>6</b>	48,891,600
<b>7</b>	51,813,019
<b>8</b>	57,456,220
<b>9</b>	<b>61,038,764</b>

Table B.2. Case study 2

<b>Number of Benches</b>	<b>Total Economic Block Values (\$)</b>
<b>1</b>	79,074
<b>2</b>	42,066
<b>3</b>	-69,586
<b>4</b>	-169,511
<b>5</b>	-51,524
<b>6</b>	-226,014
<b>7</b>	-349,878
<b>8</b>	942,861
<b>9</b>	-1,348,130
<b>10</b>	-2,131,301
<b>11</b>	2,429,466
<b>12</b>	-2,677,399
<b>13</b>	10,015,901
<b>14</b>	<b>22,706,767</b>
<b>15</b>	21,175,463
<b>16</b>	21,723,510

Table B.3. Case study 3

<b>Number of Benches</b>	<b>Total Economic Block Values (\$)</b>
<b>1</b>	-17,205
<b>2</b>	-161,866
<b>3</b>	-520,230
<b>4</b>	-1,320,581
<b>5</b>	-2,952,331
<b>6</b>	1,062,564
<b>7</b>	22,914,448
<b>8</b>	<b>35,734,525</b>

Table B.4. Case study 4

<b>Number of Benches</b>	<b>Total Economic Block Values (\$)</b>
<b>1</b>	-7,950
<b>2</b>	-85,882
<b>3</b>	-241,282
<b>4</b>	-623,646
<b>5</b>	-1,672,020
<b>6</b>	-3,387,864
<b>7</b>	6,032,261
<b>8</b>	<b>16,884,309</b>

### C. OVERALL SLOPE ANGLES AND CROSS SECTIONS

Table C.1. Overall slope angles for smaller block model (number of blocks =81,600)

Cross sections (Azimuth)				Cross sections (Azimuth)			
Input	Interpolation	Output	Absolute difference	Input	Interpolation	Output	Absolute difference
10	35	36.560	0.124	190	43-45	40.837	3.724
40	33	32.732	0.268	220	45	45	0.895
110	37	33.870	3.13	290	40-36	40	3.981
155	40	40.3	0.515	335	36	37	2.456
170	43	40	1.561	350	36	37.600	1.742
220	45	45	0.439	40	33	33	2.124
275	40	43	7.904	95	33-37	34.841	1.252
340	36	37	0.968	160	40-43	40.300	2.919

Table C.2. Overall slope angles for larger block model (number of blocks=494,900)

Cross Sections (Azimuth)					Cross Sections (Azimuth)				
Sections	Input	Interpolation	Output	Absolute difference	Sections	Input	Interpolation	Output	Absolute difference
10	35	36.560	36.110	0.450	190	43-45	40.837	40.575	0.262
40	33	33	32.973	0.027	220	45	45	44.680	0.320
110	37	36	37.520	1.52	290	40-36	40	40.506	0.506
155	40	40.3	39.486	0.814	335	36	37	35.944	1.056
170	43	40	39.375	0.625	350	36	37.600	37.146	0.454
220	45	45	44.680	0.32	40	33	33	32.973	0.027
275	40	43	42.165	0.835	95	33-37	34.841	34.490	0.351
340	36	37	35.860	1.14	160	40-43	40.300	40.506	0.206

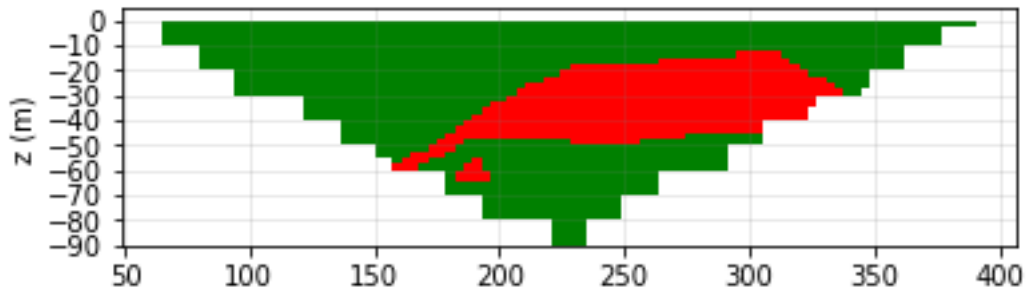


Figure C.1. N 45 E section of the extracted blocks of the magnetite orebody

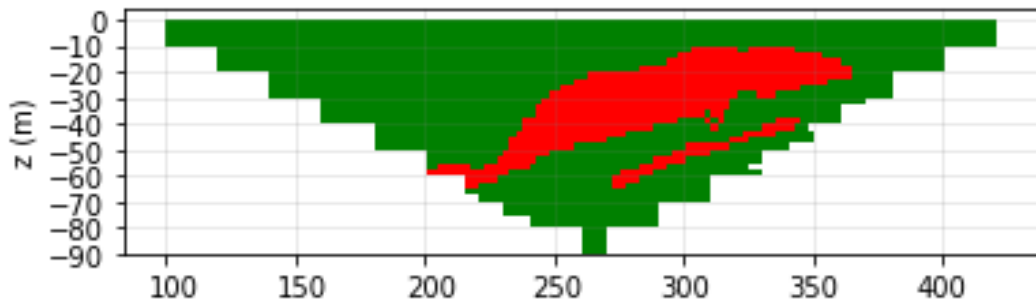


Figure C.2. W E section of the extracted blocks of the magnetite orebody

Table C.3. Comparison of overall slope angles for magnetite orebody

<b>Cross sections</b>	<b>Input</b>	<b>Measured</b>	<b>Absolute difference</b>	<b>Input</b>	<b>Measured</b>	<b>Absolute difference</b>
N S	30	30.964	0.964	30	30.548	0.548
N 45 E	30	30.051	0.051	30	30.051	0.051
W E	30	30.964	0.964	30	29.358	0.642

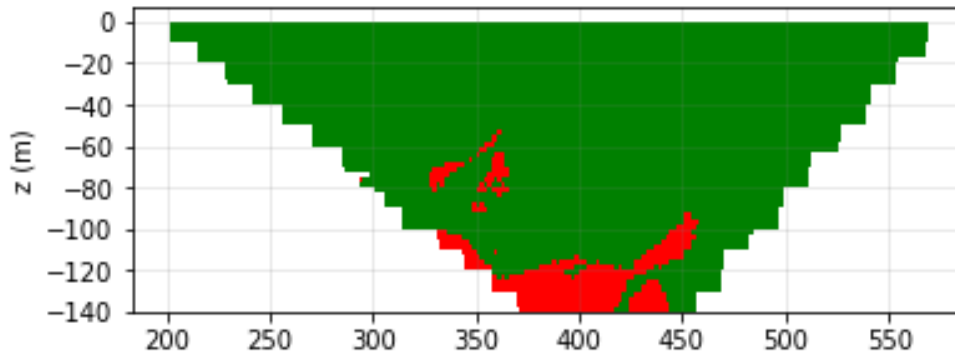


Figure C.3. S 45 E section of the extracted blocks of magnetite-hematite orebody

Table C.4. Comparison of overall slope angles for magnetite-hematite orebody

Cross sections	S 45 E			N 45 E		
	Input	Measured	Absolute difference	Input	Measured	Absolute difference
S 45 E	51	51.058	0.058	41	39.521	1.479
N 45 E	58	58.780	0.780	55	55.221	0.221



Figure C.4. N 45 E section of the extracted blocks of lignite orebody (lignite 1)

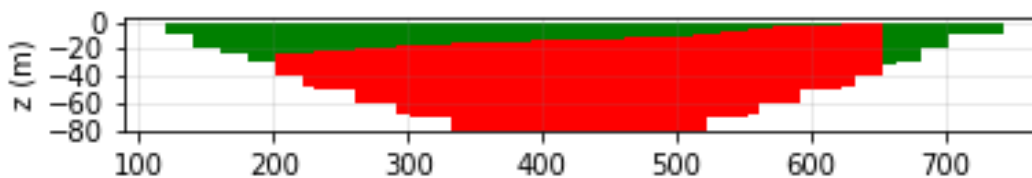


Figure C.5. W E section of the extracted blocks of lignite orebody (lignite 1)

Table C.5. Comparison of overall slope angles for lignite orebody (lignite 1)

Cross sections	Depth range	Input			Output		
		Input	Output	Absolute difference	Input	Output	Absolute difference
N S	0-40	25	23.962	1.038	25	29.745	4.745
	40-80	20	19.983	0.017	20	19.983	0.017
N 45 E	0-40	25	25.239	0.239	25	22.004	2.996
	40-80	20	19.472	0.528	20	19.472	0.528
W E	0-40	25	23.962	1.038	25	26.565	1.565
	40-80	20	19.983	0.017	20	19.983	0.017

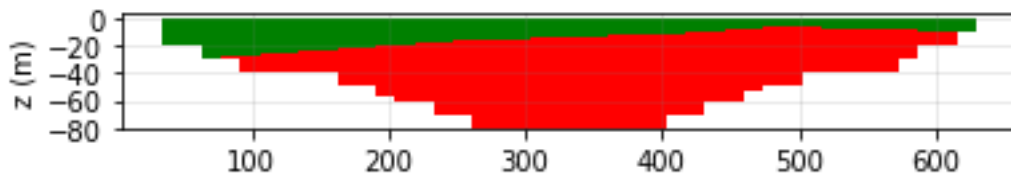


Figure C.6. S 45 E section of the extracted blocks for lignite orebody (lignite 2)

Table C.6. Comparison of overall slope angles for lignite orebody (lignite 2)

Cross section	Depth range	Input			Output		
		Input	Output	Absolute difference	Input	Output	Absolute difference
N 45 E	0-40	35	35.265	0.265	38	35.268	2.732
	40-80	25	25.240	0.240	28	29.496	1.496
S 45 E	0-40	30	35.264	5.264	31	35.264	4.264
	40-80	20	22.002	2.002	21	22.002	1.002